

CONSEQUENCES OF CLIMATE CHANGE FOR NATIVE PLANTS AND CONSERVATION



A White Paper from the California Energy Commission's California Climate Change Center

Prepared for: California Energy Commission

Prepared by: Lee Hannah, M. Rebecca Shaw, Patrick Roehrdanz, Makihito Ikegami, Oliver Soong, James Thorne

JULY 2012

CEC-500-2012-024

Lee Hannah^{1,3}
M. Rebecca Shaw²
Patrick Roehrdanz³
Makihito Ikegami³
Oliver Soong³
James Thorne⁴

¹Conservation International

²Environmental Defense Fund

³University of California, Santa Barbara

⁴University of California, Davis



DISCLAIMER

This paper was prepared as the result of work sponsored by the California Energy Commission. It does not necessarily represent the views of the Energy Commission, its employees or the State of California. The Energy Commission, the State of California, its employees, contractors and subcontractors make no warrant, express or implied, and assume no legal liability for the information in this paper; nor does any party represent that the uses of this information will not infringe upon privately owned rights. This paper has not been approved or disapproved by the California Energy Commission nor has the California Energy Commission passed upon the accuracy or adequacy of the information in this paper.

ACKNOWLEDGEMENTS

The authors would like to thank Dr. Frank Davis, Dr. David Stoms, and the Bren School of Environmental Science and Management Biogeography Lab (University of California, Santa Barbara) for valuable input regarding the species distribution modeling effort. The authors also thank Dr. Steven Phillips (AT&T Labs) for insight into the network flow analysis. Finally the authors thank Dr. Kim Nicholas (Lund University, Sweden), Dr. Josh Viers (University of California, Davis), and Dr. Greg Jones (Southern Oregon University) for guidance on the topic of viticulture and climate.

ABSTRACT

Species ranges are dynamic, and often respond to changes in global climate. Recorded increases of global average temperatures through the twentieth century have already resulted in observed shifts of species ranges within California. Projections of future species distributions under climate change are possible through models that correlate known species occurrences with observed historical climate, then project this correlation onto scenarios of climate change. Previous work in California has focused on modeling changes in the distribution of vegetation and species. This study expands on this work through (1) modeling species at finer spatial scales than previously possible, (2) applying those models in advanced conservation planning tools, and (3) illustrating the intersection of human adaptation and conservation under climate change. Section 1 presents a suite of species distribution models created with climate and water balance data that has been statistically downscaled to finer horizontal resolutions than previous statewide modeling efforts. The models encompass range simulations for over 2,000 native California plant species at scales of 90 meters, 270 meters, 800 meters, 4 kilometers, and 16 kilometers, using three time periods, two global climate models, and two emissions scenarios. Section 2 presents Network Flow Analysis that has been developed as a conservation planning tool to assess landscape connectivity for species to respond to climate change. California is a particularly challenging application for Network Flow Analysis because of its large size and diverse flora. This paper presents methods that have been developed to overcome these challenges and applied as proof-of-concept for use in California. Section 3 presents changing suitability for wine grape cultivation in California using fine-scale (270 meter) climatology. Results from this study show that projected future distributions of climates currently associated with California viticulture may result in cropping changes or other adaptive responses from wine grape growers, with potentially serious implications for land and water conservation.

Keywords: Climate change, species distribution models, protected area connectivity, non-analogue communities, agriculture

Hannah, Lee, M. Rebecca Shaw, Makihiko Ikegami, Patrick R. Roehrdanz, Oliver Soong, and James Thorne. 2012. *Consequences of Climate Change for Native Plants and Conservation*. California Energy Commission. Publication number: CEC-500-2012-024.

TABLE OF CONTENTS

Acknowledgements	i
ABSTRACT	ii
TABLE OF CONTENTS.....	iii
LIST OF FIGURES	iv
LIST OF TABLES	vi
Section 1: Fine-Scale Species Models.....	1
1.1 Introduction and Background	1
1.2 Methods	2
1.2.1 Fine-scale Climatologies.....	2
1.2.2 Species Distribution Model - Maxent.....	2
1.2.3 Species Occurrence Data	5
1.2.4 Environmental Layers	5
1.3 Results.....	8
1.3.1 SDM Database	8
1.3.2 Relative Contribution of Environmental Layers	9
1.3.3 Effect of Scale on Range Projections	10
1.3.4 Example Application: Modeled Native Species Richness	12
1.4 Discussion	16
1.5 Conclusions.....	17
Section 2: A New Conservation Planning Tool for Identifying Landscape Connectivity for Climate Change	18
2.1 Introduction	18
2.2 Methods	19
2.3 Results.....	20
2.4 Discussion	27
2.5 Conclusions.....	28
Section 3: Impacts on Plant Communities of Changes in Viticulture	29
3.1 Introduction	29
3.1.1 Background	29

3.1.2 Previous Work Linking Climate to Viticulture.....	29
3.1.3 Novel Aspects of this Study	30
3.2 Methods.....	30
3.2.1 Viticulture Suitability Models	30
3.2.2 Climate Data	32
3.2.3 Viticulture Occurrence Points	33
3.2.4 Protected Area Mask	33
3.2.5 Soils and Topography.....	33
3.3 Results.....	34
3.3.1 Future Projections of Optimal Viticulture Climates within California	34
3.3.2 Global Context.....	38
3.4 Potential Conservation Impacts	40
3.5 Conclusions.....	42
References.....	43
Glossary	48

LIST OF FIGURES

Figure 1.1: Sample Maxent Model for Present Distribution of <i>Quercus Lobata</i> . Warm colors indicate greater probability of species occurrence whereas cooler colors indicate lower probability. Species occurrence points used in building the model are depicted by white squares.	3
Figure 1.2: Sample Maxent Output Plot of Model Sensitivity vs. 1 – Specificity. In this paper, the equal sensitivity plus specificity is used as a threshold to produce binary range maps from continuous value Maxent model output.	3
Figure 1.3: A Sample Binary Range Map Produced from the Maxent Model Shown in Figure 1.1. An equal sensitivity plus specificity logistic threshold is applied to produce the binary map.	4
Figure 1.4: Example Output of Binary Maxent Species Distribution Model for <i>Quercus lobata</i> Using GFDL Climate Projections for Mid-century (2041–2070) under A2 Emissions Scenario at Two Different Horizontal Resolutions (A) 4 km; (B) 270 m. In all panels, Red = Present range lost by mid-century; Yellow = Novel range by mid-century; Green = Range retained in both time periods.	5
Figure 1.5: Dendrogram of Bioclimatic Parameters for Global Mediterranean Regions. Cluster analysis was used to generate the distances among the component loadings of each parameter	

from Principal Components Analysis. This analysis was then used to guide the selection of bioclimatic parameters used in species distribution models for California plant species.....	7
Figure 1.6: Plot of Mean Ratio of Current Area to Projected Future Area for All Modeled Species under PCM 2070–2099 A2 Climate Emissions Scenario. X-axis is horizontal grid cell size. Error bars are 95% confidence intervals.....	11
Figure 1.7: Boxplot of Percent Current Range Lost for All Modeled Species under the PCM 2070–2099 A2 Climate Emissions Scenario. X-axis is horizontal grid cell size.....	12
Fig 1.8: Spatial Distribution of Disagreement between 800 m and 270 m Species Distribution Models for PRISM 1971–2000 Climate. High disagreement (deep blue on color ramp) represents disagreement of approximately 5%–10% of modeled species.	12
Figure 1.9: Modeled Native Species Richness as Determined by Summed 800 m Resolution Binary Range Maps Produced with PRISM 1971–2000 Climate Data	14
Figure 1.10: Modeled Native Species Richness as Determined by Summed 800 m Resolution Binary Range Maps Produced under the A2 emissions scenario for 2071–2100. Panel A = GFDL; Panel B = PCM.....	15
Figure 1.11: Change in Modeled Species Richness from Current Climate to 2071–2100 A2 emissions scenario. Light colors (Yellow to Orange) show decline in species richness and darker colors (Pink to Deep Blue) show an increase in modeled richness. Panel A = GFDL; Panel B = PCM.....	15
Figure 1.12: Range-size rarity weighted species richness. Each modeled binary distribution is given a weight that is the inverse of the modeled area (narrowly distributed species are given greater weight). Panel A = Current Climate (PRISM data); Panel B = 2071–2100 (PCM data; A2 emissions scenario).	16
Figure 2.1: Illustration of Chains of Suitable Habitat. Regions shaded blue represent suitable habitat in each time step on a 3 x 3 grid. Grey arrows represent possible chains within a species dispersal capability necessary to retain suitable habitat in all time steps.....	19
Figure 2.2: Number of species that fail suitable habitat requirements (left panel) and total sites selected for additional protection (right panel) by dispersal distance assumption. Each series represents a GCM (PCM or GFDL), time period (through 2050 or 2080), and suitable habitat requirement (100 km ² or 1,000 km ²) combination.	21
Figure 2.3: Number of species that fail suitable habitat requirements (left panel) and total sites selected for additional protection (right panel) by GCM. Each series represents a dispersal assumption (0, 1.5, or 2.5 pixels), time period (through 2050 or 2080), and suitable habitat requirement (100 km ² or 1,000 km ²) combination.	21
Figure 2.4: Depiction of Areas Required to Form Chains of Protection through 2050 – GFDL, A2 Emissions Scenario; 2.5 Cell/Decade Dispersal Assumption.....	22
Figure 2.5: Depiction of Areas Required to Form Chains of Protection through 2080 – GFDL, A2 Emissions Scenario; 2.5 Cell/Decade Dispersal Assumption.....	23
Figure 2.6: Depiction of Areas Required to Form Chains of Protection through 2050 – PCM, A2 Emissions Scenario; 2.5 Cell/Decade Dispersal Assumption.....	23

Figure 2.7: Depiction of Areas Required to Form Chains of Protection through 2080 – PCM, A2 Emissions Scenario; 2.5 Cell/Decade Dispersal Assumption.....	24
Figure 2.8: Illustrative Focal Areas for Climate Change Connectivity. Regions in blue are polygons enclosing clusters of connectivity chains presented in Figure 2.8. Lists of species responsible for the required chains in each focal area are presented in Table 2.1.....	25
Figure 2.9: Required chains of <i>Salvia leucophylla</i> (blue) overlaid on all connectivity chains formed under GFDL climate projections through 2080. Model outputs shown assume 1.5 pixel dispersal distance and 1,000km ² suitable habitat (57 chains) requirement.	27
Figure 3.1: Modeled Distributions of Suitable Climates for Viticulture under the A2 Emissions Scenario for Three Time Periods: 1971–2000 (Red); 2040–2070 (Orange); 2070–2100 (Blue). Light Green shows suitability retained through 2070, and Dark Green denotes suitability retained through 2100. Distributions in each time period represent a consensus agreement of three suitability models: (1) mean growing season temperature, (2) maturity grouping heat summation, and (3) Maxent. The Maxent models used in this scenario are built on California viticulture occurrence points and topoclimate + soil predictor variables.	36
Figure 3.2: Modeled Distributions of Suitable Climates for Viticulture under the A2 Emissions Scenario for Three Time Periods Using Global Viticulture Occurrence Points: 1971–2000 (Red); 2040–2070 (Orange); 2070–2100 (Blue). Light Green shows suitability retained through 2070 and Dark Green denotes suitability retained through 2100. Distributions in each time period represent a consensus agreement of three suitability models: (1) mean growing season temperature, (2) maturity grouping heat summing, and (3) Maxent. The Maxent models used in this scenario are built on global viticulture occurrence points and topoclimate-only predictor variables.	37
Figure 3.3: Climate Change Impacts on Viticulture Suitability Are Illustrated for Three Time Periods (Present, 2050, and 2090) Based on a Consensus Approach Using Multiple Suitability Models and an Ensemble Projection of Future Climate under the A2 Emissions Scenario (IPCC AR4). Broad areas of current suitability are lost by 2050 in all major wine-producing regions (red). Large areas of new suitability (2050 orange; 2090 blue) open in Northern Europe and North America. Insets A–E show regional detail. Areas where viticulture is retained through mid-century and through all three time periods are shown as light green and dark green, respectively.	39
Figure 3.4: Potential Conflict of Natural Areas and Optimal Viticulture Climates. Areas where optimal viticulture climate modeled for all periods (Current, 2041–2070, and 2071–2100) intersects with National Land Cover Dataset (NLCD) 2001 undeveloped land shown in black. Suitable areas for viticulture that do not intersect with natural areas are shown as Current = Red; 2041–2070 = Orange; 2071–2100 = Blue. The left panel is the San Francisco Bay Area north to Humboldt County, and the right panel is the Bay Area south to Ventura County.	41

LIST OF TABLES

Table 1.1: Summary of SDMs Produced	8
---	---

Table 1.2: Mean Variable Contribution across all SDM by Scale. Values are percent contribution. Bio_4 = Temperature seasonality; bio_5 = Maximum temperature of warmest month; bio_6 = Minimum temperature of coldest month; bio_15 = Precipitation seasonality; bio_18 = Precipitation of warmest quarter; bio_19 = Precipitation of coldest quarter; bio_20 = Cumulative growing degree days above 5°C; bio_24 = Aridity index; ph = Soil pH; awc = Soil available water capacity; dep = Soil depth.....	9
Table 2.1: List of Species Contributing to Required Chains in Illustrative Focal Areas	26
Table 3.1: Change in Climates Currently Associated with Viticulture in California. Negative values of change can be interpreted as the percent of currently suitable land that will require adaptation measures for continued viticulture.	36
Table 3.2: Change in Climates Currently Associated with Viticulture by County using Global Viticulture Occurrence Points and A2 Emissions Scenario. Negative values of change can be interpreted as the percent of currently suitable land that will require adaptation measures for continued viticulture.	37
Table 3.3: Projected Loss of Currently Suitable Area and the Ratio of Total Future Suitability to Current Suitability in Select Wine-Producing Regions – A2 Emissions Scenario.....	40
Table 3.4: Summary of Climate Change Effects on the Total Optimal Viticulture Area in Non-natural Lands and the Ratio of Viticulture Climates in Natural to Non-natural Lands.....	42

Unless otherwise noted, all tables and figure are provided by the author.

Section 1: Fine-Scale Species Models

1.1 Introduction and Background

Previous assessment work in California has focused on modeling of changes in the distribution of vegetation types and species. These analyses have been conducted at scales of kilometers. Recent advances in climate downscaling now make it possible to implement species models at sub-kilometer scales. Yet coarser-scale models remain relevant for statewide assessment, where fine-scale models become computationally intensive. We therefore have modeled California native plant species for this assessment at multiple scales: 90 meters (m), 270 m, 4k m, and 16 kilometers (km). The 90 m modeling is over 100 times finer resolution than the previous 1 km-scale state assessment species models. The remainder of this introduction presents the history of species modeling, its rationale, the development of fine-scale modeling techniques, and the importance of fine-scale models.

Species' responses to temperature increases have already resulted in observed shifts of species' ranges both poleward and upward along elevational gradients (Parmesan 2006). Recent research provides empirical evidence of shifting species ranges. Kelly and Goulden (2008) compared 1977 and 2006–2007 plant cover surveys along a 2,314 m elevation gradient in the Santa Rosa Mountains of Southern California. The study found that the elevation of the dominant plant species rose by an average 65 m between survey periods. Moritz et al. (2008) document an average of 500 m upward change in the range limits of small mammal species in Yosemite National Park in comparison to surveys conducted in the early twentieth century (Grinnell 1924).

California's Mediterranean habitat diversity has evolved under hot, dry summers and cool, wet winters (Ackerly 2009), but climate projections for California indicate that this climate regime may contract by up to 20 percent of current extent by 2050 (Klausmeyer and Shaw 2009). Mean annual temperatures in California have already increased by 1°C (1.8°F) between 1950 and 2000 (LaDochy et al. 2007), and in the future novel climates are expected to appear (Williams and Jackson 2007). Under the current global greenhouse gas emissions trajectory, California's average annual temperatures are projected to rise by 3.8°C–5.8°C (6.8°F–10.4°F) and annual precipitation changes may range anywhere from a decrease of 157 millimeters (mm) to an increase of 38 mm (Hayhoe et al. 2004; Cayan et al. 2008). The anticipated emergence of future climatic conditions with no current analog threatens endemic species with limited dispersal capability and/or a high degree of ecological specialization (Loarie et al. 2008; Stralberg et al. 2009).

In light of these changes, it is important to estimate the possible extent of species' range movements due to future climate change. Many researchers in California have helped pioneer modeling designed to address this question. Early results have been very useful in framing conservation problems posed by climate change and making initial efforts at designing solutions. As these efforts have matured, a variety of modeling approaches have begun to converge, with many researchers now using Maxent as their main modeling tool. Scale of modeling has become increasingly fine-grained, with 800 m horizontal resolution now common and finer-resolution models (90 m–270 m) emerging.

To produce a uniform set of species distribution models at multiple scales, this project used newly available climate data and an improved dataset of species occurrence data for 2,235 native California plant species. Modeled distributions were generated at 270 m, 800 m, 4,000 m, and 16,000 m for current climate, as well as mid-century and end-of-century projections across multiple general circulation model (GCM)/emission scenario combinations (Geophysical Fluid Dynamics Laboratory [GFDL] and Parallel Climate Model [PCM] projections; A2 and B1 Intergovernmental Panel on Climate Change's [IPCC's] Special Report on Emissions Scenarios [SRES] emissions scenarios). A limited number of species (53 total) were modeled at 90 m, as the very large datasets involved precluded running and archiving all species. The capacity to run species on demand at 90 m now exists for all 2,235 species, however. The 270 m and 90 m datasets are the largest such modeling effort at the statewide domain with this newly produced fine-scale climatology.

1.2 Methods

1.2.1 Fine-scale Climatologies

Historical climate data is based on PRISM (PRISM Climate Group, Oregon State University), and future climate data is from simulations of the GFDL (2001-2100) and PCM (2000-2099) models using A2 and B1 emission scenarios. All climate data were downscaled to 90 m and 270 m and upscaled to 4,000 m and 16,000 m by Alan and Lorrie Flint of the United States Geological Survey (USGS) (Flint and Flint 2012) and to 16,000 m by us using the aggregate function in ArcGIS (ver 9.3). From annual monthly maximum temperature, minimum temperature and precipitation data, we calculated 30-year averages for the periods of 1971–2000, 2040–2070, and 2070–2100.

1.2.2 Species Distribution Model - Maxent

Maxent 3.3.3e (Phillips and Dudik 2008) is used to generate a probability surface of species presence according to the environmental input layers (e.g., bioclimatic variables, soils) and the known locations of species occurrence. In building the predictive models presented in this paper, 70 percent of the occurrence points were used to correlate the environmental layers to observed species presence. The remaining 30 percent of occurrence points were reserved to validate the model.

Standard Maxent output is a grid of continuous values from 0 to 1 representing the statistical correlation of the environmental layers based on what is observed at each known occurrence point of a particular species. When projected over the entire model domain (Figure 1.1), this correlation may be interpreted as the probability of species occurrence at the location of a particular grid cell. To produce a binary species range map (presence vs. absence), a threshold must be applied to the raw, continuous output. For modeled distributions presented here, the “equal sensitivity and specificity logistic threshold” (Figure 1.2) generated from the model test run is used to produce a binary range map (Figure 1.3) in each time period.

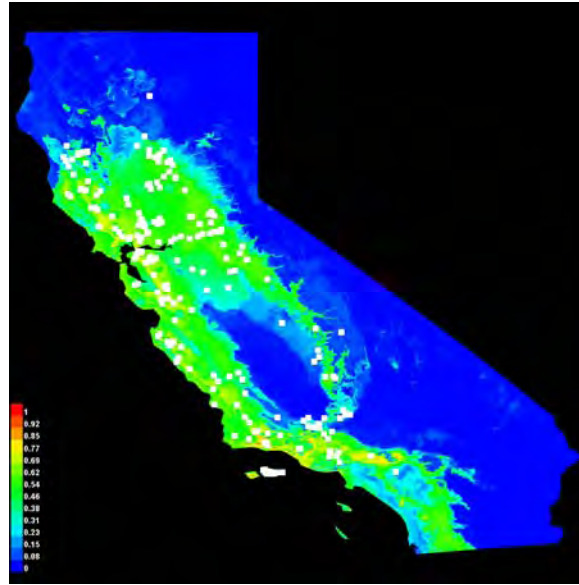


Figure 1.1: Sample Maxent Model for Present Distribution of *Quercus Lobata*. Warm colors indicate greater probability of species occurrence whereas cooler colors indicate lower probability. Species occurrence points used in building the model are depicted by white squares.

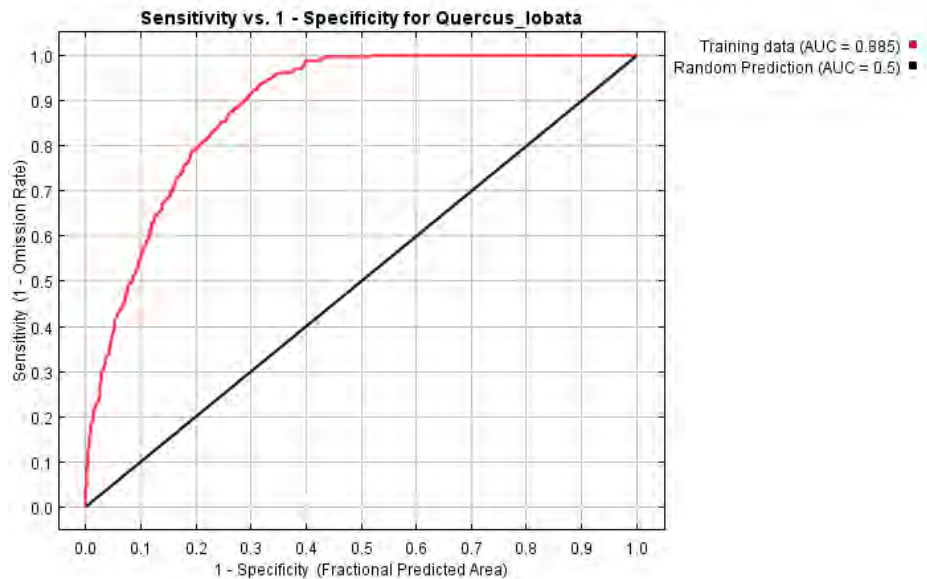


Figure 1.2: Sample Maxent Output Plot of Model Sensitivity vs. 1 – Specificity. In this paper, the equal sensitivity plus specificity is used as a threshold to produce binary range maps from continuous value Maxent model output.

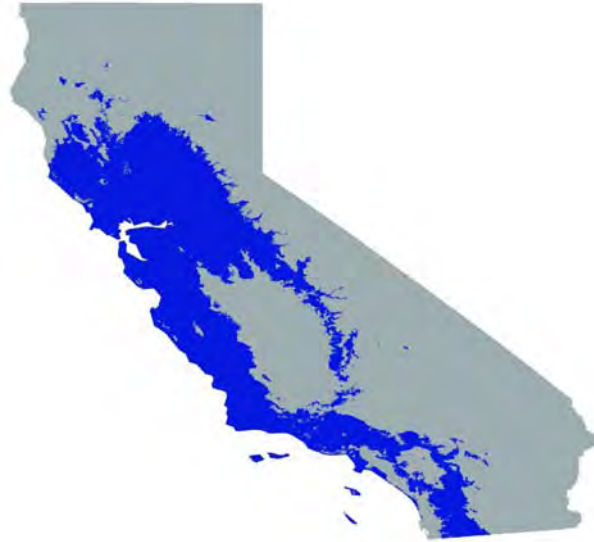


Figure 1.3: A Sample Binary Range Map Produced from the Maxent Model Shown in Figure 1.1. An equal sensitivity plus specificity logistic threshold is applied to produce the binary map.

Binary maps representing modeled distributions for each of the three time steps (1971-2000; 2040-2070; 2070-2100) may be overlaid to produce a “stoplight” map of range loss, gain, and stability (Figure 1.4). Though species’ differing abilities to adapt to climate change and the complexity of ecological processes that determine a species range (e.g., dispersal, specific soil requirements, species interactions, and population dynamics) caution against literal interpretation of modeled future distributions, the stoplight maps are instructive in that they highlight regions where a species is likely to be stressed by future climatic conditions versus regions that are comparatively stable, and therefore offer potential refugia for a species under climate change. As Section 2 will illustrate, systematically tracking potential climatic refugia through time for a large suite of species can provide insights into which regions will be important to provide the temporal connectivity that will accommodate shifting species ranges through time.

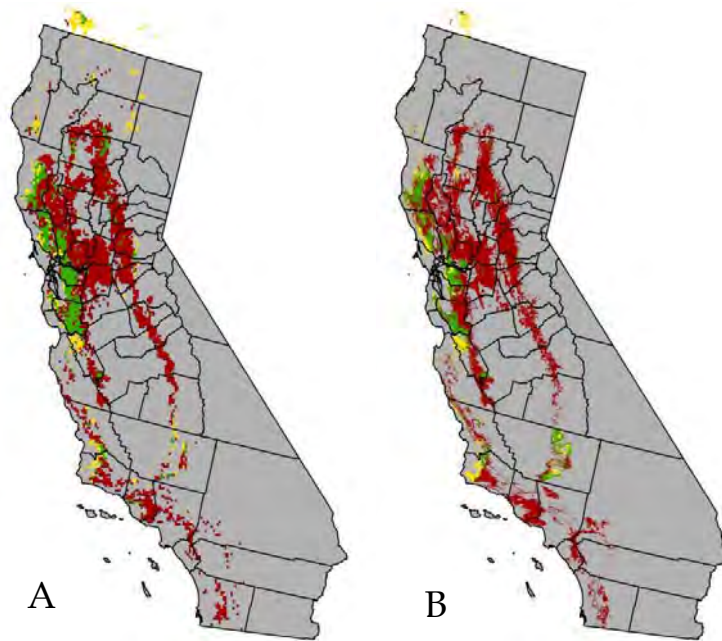


Figure 1.4: Example Output of Binary Maxent Species Distribution Model for *Quercus lobata* Using GFDL Climate Projections for Mid-century (2041–2070) under A2 Emissions Scenario at Two Different Horizontal Resolutions (A) 4 km; (B) 270 m. In all panels, Red = Present range lost by mid-century; Yellow = Novel range by mid-century; Green = Range retained in both time periods.

1.2.3 Species Occurrence Data

We used the California native and endemic plants database created at the University of California, Davis, to drive the species distribution models. The database contains point locality data from presence-only herbarium data and presence plus absence plot observation data. To minimize errors in point locality data, any points outside of known distribution by county or biological region were omitted. With these data points removed, species with more than 10 documented point locality data points were chosen for statewide modeling. It is by this process that we arrived at the list of 2,235 native California plant species suitable for modeling current and future distributions. Many species on the list are endemic to California, but a species was not necessarily omitted from the list even if the majority of its documented range lies outside of California.

1.2.4 Environmental Layers

1.2.4.1 Bioclimatic Parameters

In all species distribution models, eight bioclimatic variables calculated from monthly climatic data were used as predictor environmental layers. All bioclimatic parameters represent 30-year averages from the modeled time periods (1971–2000, 2040–2070, and 2070–2100). The bioclimatic parameters used in building species distribution models were:

- Temperature Seasonality (bio_4)
- Maximum Temperature of Warmest Month (bio_5)
- Minimum Temperature of Coldest Month (bio_6)
- Precipitation Seasonality (bio_15)

- Precipitation of Warmest Quarter (bio_18)
- Precipitation of Coldest Quarter (bio_19)
- Cumulative Growing Degree Days above 5°C (bio_20)¹
- Aridity Index (bio_24)² – Aridity is defined as total annual precipitation/potential evapotranspiration

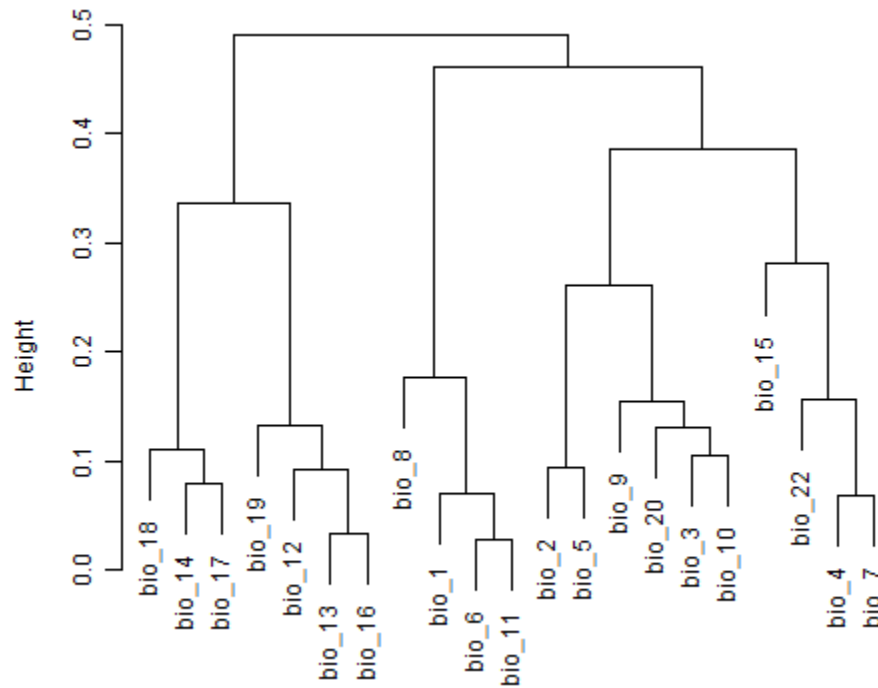
This list of parameters was chosen in part by virtue of a principal component analysis (PCA) conducted over global Mediterranean climate regions. To capture a range of potential climatic predictor variables without appreciable correlation, we chose parameters that were likely to have readily identified, meaningful biological effects (e.g., Minimum Temperature of Coldest Month) and were less closely grouped on the PCA dendrogram (Figure 1.5). We also included Aridity Index because it combines climate variables with surface topology parameters (i.e., slope and aspect) that are expected to be important in determining species ranges at finer resolutions. Slope and aspect were calculated from digital elevation model (DEM) data at each scale using ArcGIS spatial tools.

¹ Cumulative Growing Degree Days (GDD) are an accumulation of average temperature above a base temperature (5°C).

$$GDD5 = \sum_{i=1}^{12} \left[\left(\frac{T_{min_i} + T_{max_i}}{2} \right) - 5 \right] D_i$$

where $T_{min}(i)$ and $T_{max}(i)$ are average minimum and maximum temperatures for month i and D is the number of days in month i . When $T_{min}(i) < 5^\circ\text{C} < T_{max}(i)$, we adjust the number of days in the month using $D^* = D(T_{max} - 5) / (T_{max} - T_{min})$.

² *Aridity Index* is a quotient of annual precipitation divided by potential evaporation. In this study the potential evaporation was calculated from received radiation and temperature using the methodology presented in Kay et al. (2008). Because we use slope and aspect to calculate received radiation, terrain affects Aridity Index.



Bio_1 = Annual Mean Temperature
 Bio_2 = Mean Diurnal Range (Mean of monthly (max temp - min temp))
 Bio_3 = Isothermality (BIO2/BIO7) (* 100)
 Bio_4 = Temperature Seasonality (standard deviation *100)
 Bio_5 = Max Temperature of Warmest Month
 Bio_6 = Min Temperature of Coldest Month
 Bio_7 = Temperature Annual Range (BIO5-BIO6)
 Bio_8 = Mean Temperature of Wettest Quarter
 Bio_9 = Mean Temperature of Driest Quarter
 Bio_10 = Mean Temperature of Warmest Quarter
 Bio_11 = Mean Temperature of Coldest Quarter
 Bio_12 = Annual Precipitation
 Bio_13 = Precipitation of Wettest Month
 Bio_14 = Precipitation of Driest Month
 Bio_15 = Precipitation Seasonality (Coefficient of Variation)
 Bio_16 = Precipitation of Wettest Quarter
 Bio_17 = Precipitation of Driest Quarter
 Bio_18 = Precipitation of Warmest Quarter
 Bio_19 = Precipitation of Coldest Quarter
 Bio_20 = Cumulative Growing Degree Days above 5°C (41°F)
 Bio_22 = Precipitation as snow

Figure 1.5: Dendrogram of Bioclimatic Parameters for Global Mediterranean Regions. Cluster analysis was used to generate the distances among the component loadings of each parameter from Principal Components Analysis. This analysis was then used to guide the selection of bioclimatic parameters used in species distribution models for California plant species.

1.2.4.2 Soil Parameters

In addition to the bioclimatic parameters described above, we used the State Soil Geographic database (STATSGO2) data for soil parameters. We matched the database to polygons of generalized soil types to generate predictor environmental layers of available water capacity, pH, and soil depth. Soil-type data used to generate the species distribution models (SDM) is available from:

(http://www.soilinfo.psu.edu/index.cgi?soil_data&conus&data_cov&awc&methods).

Soil-type polygons were converted, in each case, to the resolution of the bioclimatic parameters used to create the climate projections. Soil parameters used in this analysis are uniform within each generalized polygon. The downscaling techniques used to produce fine-scale surfaces of the bioclimatic parameters do not similarly result in greater resolution of soil variation.

1.3 Results

1.3.1 SDM Database

The result of this component of the analysis is an archived database of range distributions in present climate and range shifts under future climate scenarios. The entire database consists of more than 50,000 SDM that encompass over 2,000 native California plant species; 1971–2000, 2040–2070, and 2070–2100 time periods; GFDL and PCM climate models; A2 (business-as-usual scenario) and B1 (assumes greenhouse gas abatement by mid-century) emissions scenarios as defined by the IPCC's SRES 4. The climate projections used to develop the SDM are at scales of 90 m, 270 m, 800 m, 4 km, and 16 km (Table 1.1).

Researchers contributing to other papers in this series and to local conservation and climate change projects have already begun to use these outputs. The database is archived on storage resources provided by the Earth Research Institute at the University of California Santa Barbara. A web-based distribution portal that will allow users to query the dataset by species, GCM, emissions scenario, time period, and scale is in development. Please contact Lee Hannah at l.hannah@conservation.org for immediate access to any portion of the dataset.

Table 1.1: Summary of SDMs Produced

	16 km	4 km	800 m	270 m	90 m
GCMs	GFDL	GFDL	GFDL	GFDL	GFDL
	PCM	PCM	PCM	PCM	PCM
No. Species	2,235	2,235	2,235	2,235	53
Time Periods	1971–2000	1971–2000	1971–2000	1971–2000	1971–2000
	2040–2070	2040–2070	2040–2070	2040–2070	2040–2070
	2070–2100	2070–2100	2070–2100	2070–2100	2070–2100
Total File Size	1.7GB	6.5GB	133GB	967GB	5GB

Potential studies that make use of this dataset are wide ranging across the fields of ecology, biogeography, botany, and conservation planning. Sections 2 and 3 in this paper demonstrate three such the applications of the dataset through the investigation of areas important for temporal connectivity of climatically suitable habitat under climate change and fine-scale modeling of climates associated with premium viticulture in California. Here, we present a brief analysis of the characteristics of the dataset, including the relative predictive contribution of bioclimatic and soil parameters, modeled species richness, and the effect of scale on the systematic projection of species range shifts under climate change.

1.3.2 Relative Contribution of Environmental Layers

The selection of environmental layers used in building the model has a significant impact on the projected species ranges, particularly for end-of-century projections. The relative contribution or importance of each environmental layer to the model is available as part of the full Maxent output. Parameter contribution is variable across species and individual model iteration, but general trends are apparent (Table 1.2). For example, the variables with consistently greatest mean model contribution across all scales were Cumulative Growing Degree Days above 5°C (bio_20), Precipitation seasonality (bio_15), and Aridity Index (bio_24). Conversely, the soil parameters included in the models offer consistently lesser mean contribution.

Table 1.2: Mean Variable Contribution across all SDM by Scale. Values are percent contribution.
Bio_4 = Temperature seasonality; bio_5 = Maximum temperature of warmest month; bio_6 = Minimum temperature of coldest month; bio_15 = Precipitation seasonality; bio_18 = Precipitation of warmest quarter; bio_19 = Precipitation of coldest quarter; bio_20 = Cumulative growing degree days above 5°C; bio_24 = Aridity index; ph = Soil pH; awc = Soil available water capacity; dep = Soil depth

	bio_4	bio_5	bio_6	bio_15	bio_18	bio_19	bio_20	bio_24	ph	awc	dep
270 m	10.22	4.93	7.99	12.48	9.14	7.83	16.08	12.32	6.05	6.07	6.73
800 m	10.05	4.73	8.04	13.45	9.12	6.51	15.73	13.85	6.00	5.94	6.57
4,000 m	10.42	4.91	8.31	13.12	8.50	6.43	15.60	13.40	6.73	7.05	5.53
16,000 m	8.56	5.75	8.50	12.11	9.47	6.56	12.69	12.17	9.89	8.82	5.48
All Scales	9.82	5.08	8.21	12.79	9.06	6.84	15.04	12.94	7.15	6.96	6.08

It is unexpected that Aridity Index (bio_24), which includes slope and aspect from DEM data, declines in contribution at the finest (270 m) scale, which would theoretically offer the greatest representation of the topo-climatic processes that are known to govern species distributions at local scales. Further investigation into the variable contribution by functional grouping (e.g., trees, shrubs) or habitat type (e.g., mixed conifer, oak woodland) would offer further insight into the relative predictive value of the bio-climatic parameters, and which parameters may be most important in refining a modeled distribution for a particular species.

1.3.3 Effect of Scale on Range Projections

The fine-scale climate data used in this analysis allow the development of species models that capture topographic influences that control climate at biologically relevant scales. A primary motivation of creating the SDM products presented in this paper was to incorporate the progressive downscaled climate data with the aim of refining projections of future species distributions under climate change. The emergence of fine-scale climate data creates a tradeoff between theoretical accuracy gained through finer resolution and computational resources. It also raises the possibility that different scales may produce systematically different results in terms of the proportion of a species' range that is projected to be lost, gained, or remain stable under climate change. This in fact would be expected if fine-scale models are superior in representing the microclimates that actually control plant distributions.

Assessing the effect of scale is therefore an important application of the fine- to coarse-scale modeling conducted for this study. While the effect of scale has been addressed in the literature over various spatial domains, the few results available offer contradictory results (e.g., Randin et al. 2009; Trevidi et al. 2008). For studies specific to California plants, Seo et al. 2009 demonstrated increased utility for SDMs downscaled to 1 km as coarser resolutions (>16 km) systematically over-predicted species ranges; and thus potentially misrepresent the proportion of a species range that is stable under climate change. This problem of over-prediction was particularly evident in species with intermediate range sizes.

Here we present an overview of how binary range projections for this dataset vary according to the resolution (scale) of the climate data used to build the model. Figure 1.6 shows the mean ratio of current modeled area to projected future (2070–2099) area within California for each of the four scales available for the entire species list. Differences among the scales 270 m–4 km are generally within the 95 percent confidence interval. Models constructed with 16 km data do show a systematically lower current/future area. Figure 1.7, which illustrates the mean percent of current area lost for each scale, also shows remarkable consistency among scales 270 m–4 km, with 16 km again showing slightly more pronounced range shifts. It is important to note that the results presented in Figures 1.6 and 1.7 are aggregated across all 2,235 species. Model projections of an individual species may differ among scales in a manner that is significant for the continued management of that species. Preliminary research by a group at the University of California (UC) Santa Barbara and Arizona State University shows that these differences may be especially important for species with narrow ranges.

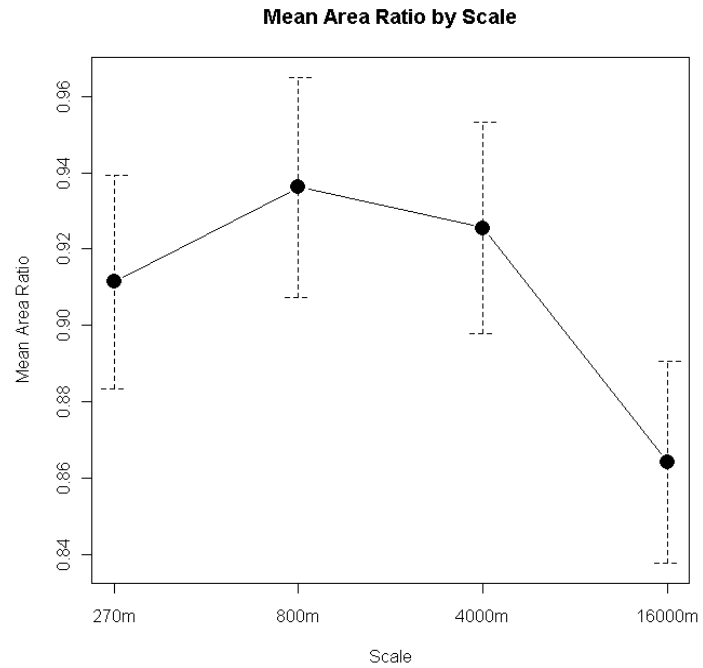


Figure 1.6: Plot of Mean Ratio of Current Area to Projected Future Area for All Modeled Species under PCM 2070-2099 A2 Climate Emissions Scenario. X-axis is horizontal grid cell size. Error bars are 95% confidence intervals.

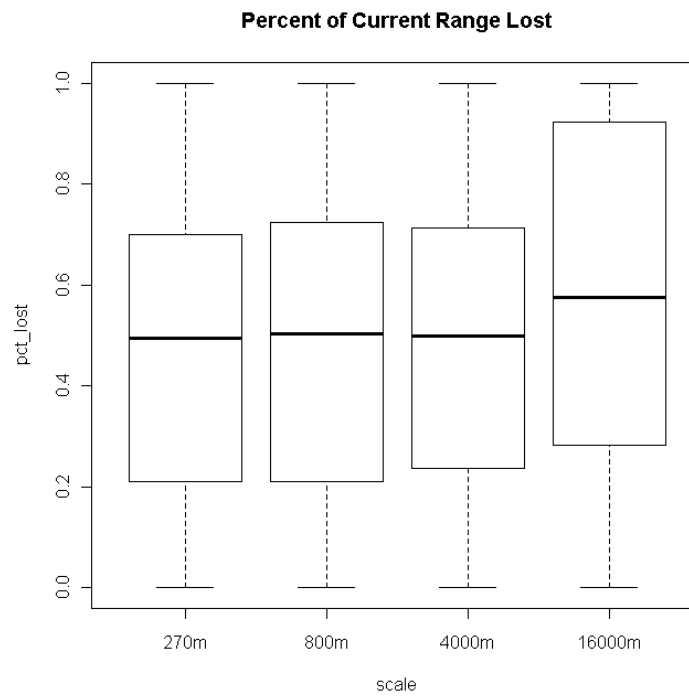


Figure 1.7: Boxplot of Percent Current Range Lost for All Modeled Species under the PCM 2070–2099 A2 Climate Emissions Scenario. X-axis is horizontal grid cell size.

To investigate whether the modeled distributions between SDMs created with 270 m and 800 m climate data show any systematic spatial pattern of disagreement, binary difference maps (where distribution agreement = 0; disagreement = 1) were created for all species in 270 m resolution. Summing the difference maps provides a total count of disagreement within each pixel. Figure 1.8 therefore shows the proportion of modeled species for which there is disagreement between the 270 m and 800 m models. In general, there is good agreement among the two scales, as the maximum disagreement values are around 5 to 10 percent of modeled species. With the exception of possible edge effects near the domain boundaries, Figure 1.8 shows no discernible systematic spatial pattern to the disagreement between the two scales.

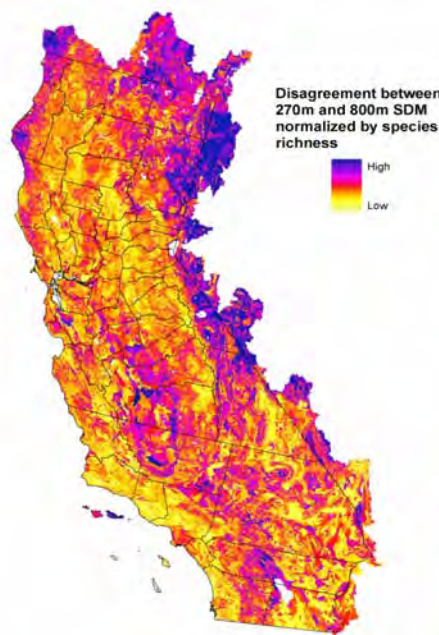


Fig 1.8: Spatial Distribution of Disagreement between 800 m and 270 m Species Distribution Models for PRISM 1971–2000 Climate. High disagreement (deep blue on color ramp) represents disagreement of approximately 5%–10% of modeled species.

1.3.4 Example Application: Modeled Native Species Richness

One application of the suite of SDM produced for this paper is to use the binary range maps to model species richness of native plants in California. *Species richness* is the total count of species that are known to occur at a given site. In the case of the SDM dataset, it is the total count of species “presence” that occurs in each pixel of the model. As a simple metric of diversity, unweighted species richness does not take into account the relative abundance or evenness among the assemblage of species that is modeled to occur in each pixel and therefore has limited value in terms of priority setting for biodiversity conservation. However, modeling species richness through time can provide an overview of the systematic trends in the modeled species range

shifts under climate change. It can also serve to highlight regions of California that are more likely to lose species richness, as well as areas that could potentially gain species due to enhanced suitability in future climates.

Figures 1.9 through 1.11 depict the modeled shift of native species richness under climate change (A2 emissions scenario). Figure 1.9 shows species richness in current climate with the general pattern of species richness in montane regions and the comparatively species-poor desert and central valley, conforming to expectations. By the end of the twenty-first century (Figure 1.10), zones of greatest species richness have contracted upslope, with greatest richness confined to the highest ridges of the Sierra Nevada mountains. Regions of California that show the greatest decline of species richness by the end of the century include the Coast and Transverse ranges, as well as the transition zone between the Central Valley and the high Sierra. This aggregate spatial pattern of species range shifts is important to recognize in planning for conservation of species under climate change. Section 2 in this paper will more thoroughly investigate which regions will be important to ensure spatio-temporal connectivity of suitable climates for all 2,235 modeled species. Finally, as an alternate metric, Figure 1.12 shows species richness that is weighted by the inverse of the modeled range size, and in doing so highlights areas that harbor rare or narrowly distributed species.

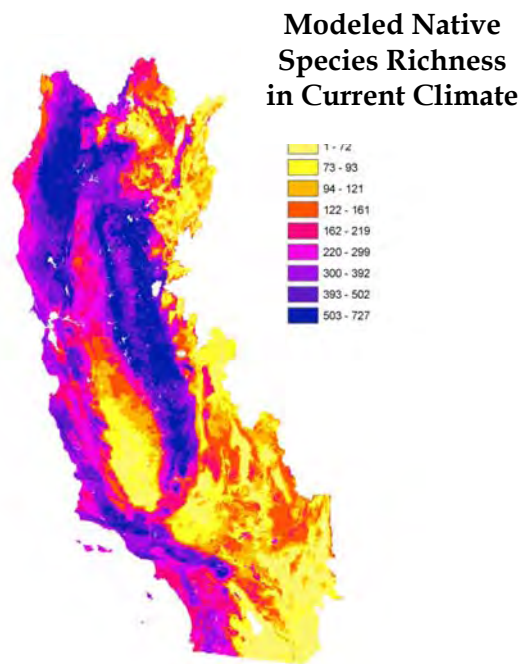


Figure 1.9: Modeled Native Species Richness as Determined by Summed 800 m Resolution Binary Range Maps Produced with PRISM 1971–2000 Climate Data

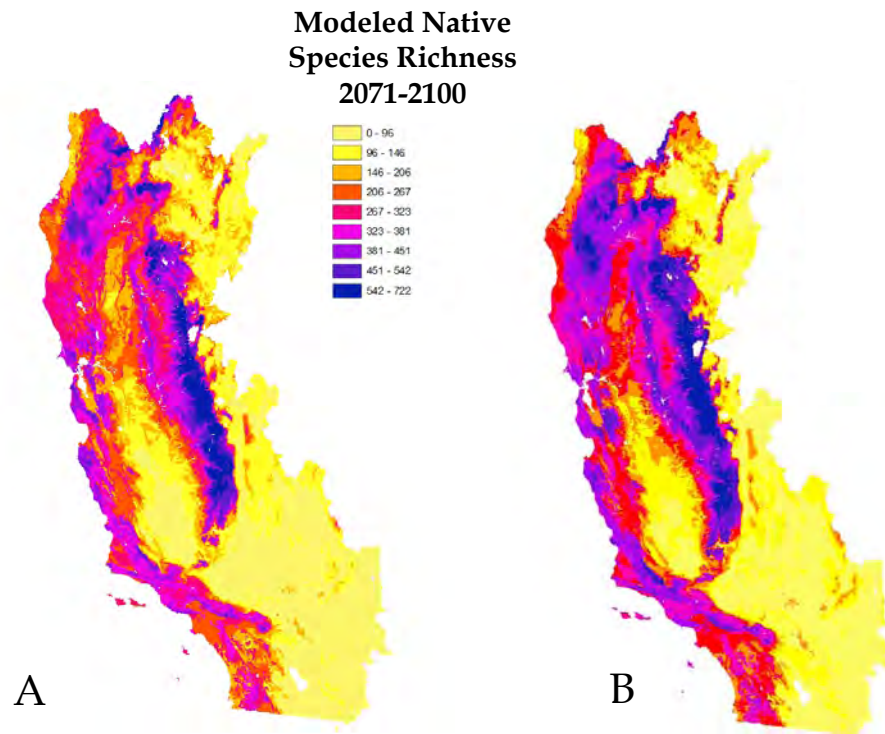


Figure 1.10: Modeled Native Species Richness as Determined by Summed 800 m Resolution Binary Range Maps Produced under the A2 emissions scenario for 2071–2100. Panel A = GFDL; Panel B = PCM.

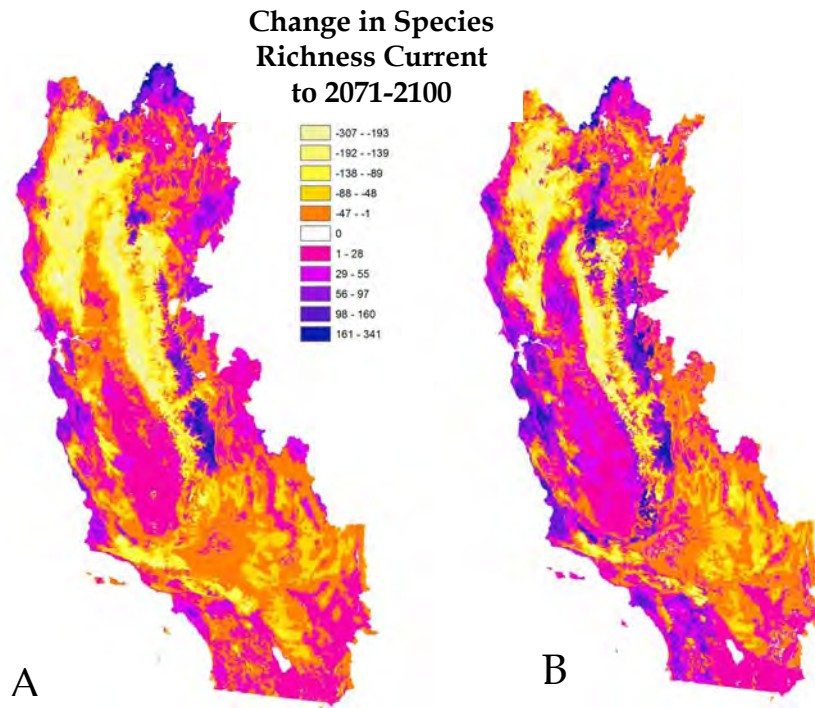


Figure 1.11: Change in Modeled Species Richness from Current Climate to 2071–2100 A2 emissions scenario. Light colors (Yellow to Orange) show decline in species richness and darker colors (Pink to Deep Blue) show an increase in modeled richness. Panel A = GFDL; Panel B = PCM.

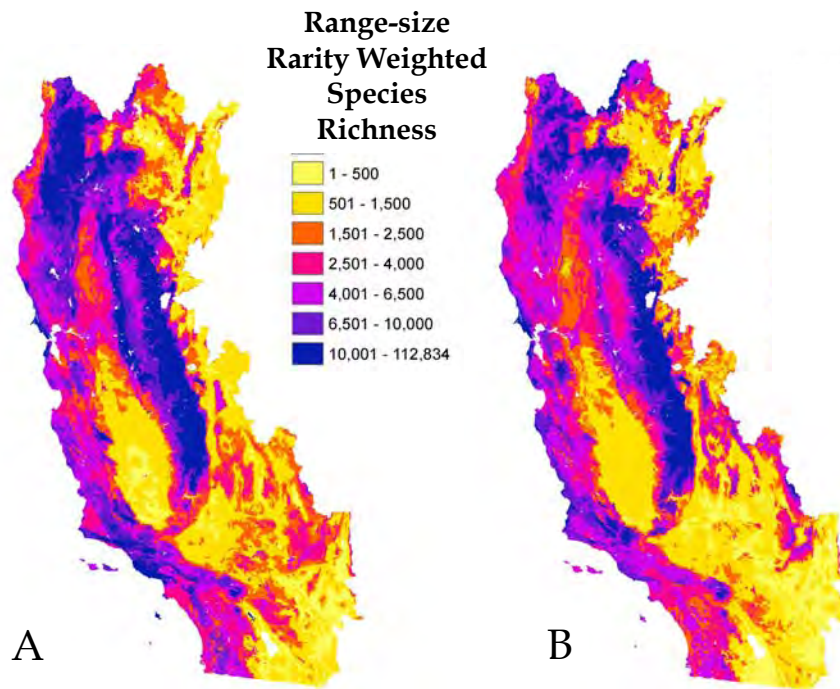


Figure 1.12: Range-size Rarity Weighted Species Richness. Each modeled binary distribution is given a weight that is the inverse of the modeled area (narrowly distributed species are given greater weight). Panel A = Current Climate (PRISM data); Panel B = 2071–2100 (PCM data; A2 emissions scenario).

1.4 Discussion

As with any modeling effort, the suite of SDM presented here rests upon a series of assumptions and decision points that shape the precise character of the modeled distributions (Wiens et al. 2009). The choice of SDM, climate data, soil data, species occurrence data, GCM projection, emissions scenario, binary thresholding method, spatial resolution, spatial domain, temporal resolution, and choice of predictor variables all contribute data quality considerations and uncertainty to the resulting model outputs (for a full discussion, see Franklin 2009). It has been demonstrated that the choice of model algorithm and predictor variables included in the model can produce radically disparate projections for the same species, even if the models are constructed with identical occurrence points (e.g., Pearson et al. 2006). Indeed, the spread in the projections produced by different SDM algorithms has been observed to be greater than the spread caused by GCM alone, rendering SDM methods a potentially greater source of uncertainty than climate projections (Araujo et al. 2005).

Although improvements in SDM methodology and the emergence of models that incorporate machine learning (e.g., Maxent used here) have resulted in greater model performance (Elith et al. 2006), there remain important differences in the ways each model handles the data inputs that must be taken into account when interpreting model projections (Elith and Graham 2009). As a means of reducing uncertainty in SDM, there have been calls to produce consensus outputs averaged from an ensemble of several models (Araujo and New 2007) and improved metrics of

predictor variable importance or ecological causal relationship (Araujo and Guisan 2006), and to further develop process-based models (e.g., Biomove, Midgley et al. 2010) or models that incorporate population dynamics (Keith et al. 2008).

Although managers, policy makers, scientists, and other consumers of SDM data must be cognizant of the uncertainties of SDM, those uncertainties must be weighed against the option of operating in the absence of the best information available (Wiens et al. 2009). The SDM presented here have been developed with the most comprehensive occurrence data, fine-scale climate and soils data, and a high-functioning but widely available SDM algorithm; and with careful selection of predictor variables that drive the projections. This suite of SDM represents a valuable and comprehensive reference dataset for use in a variety of conservation planning applications (e.g., Biomove, Network Flow Analysis) and further investigation into the effects of scale or choice of bioclimatic parameters on species distribution. It may also be used as a basis on which future refinements of SDM may be evaluated.

1.5 Conclusions

The SDM dataset presented here represents the most extensive distribution modeling effort for California plants and represents the convergence of updated species occurrence data, recently developed fine-scale climate data, and cutting-edge SDM techniques. Analysis and application of this dataset has already commenced among several research groups, which will contribute substantially to our knowledge base and collective understanding of potential climate change impacts on native and endemic California plant species.

Section 2:

A New Conservation Planning Tool for Identifying Landscape Connectivity for Climate Change

2.1 Introduction

California state climate change assessments have focused on models of vegetation types and individual species and their properties over a decade. This work has provided the raw material for improved conservation plans for climate change. Yet conservation planning tools themselves need to be updated for climate change, since most were created under the assumption of a stable climate.

An urgent need is for conservation planning tools that allow identification of landscape connectivity to support species movements in response to climate change. This section describes the development of one such tool, and its application to California. The results of this work demonstrate the utility and functionality of this new tool. The spatial results of the analysis are preliminary and have been produced primarily as proof of concept for the new tool. Many refinements will be required before final spatial recommendations can be generated. However, these early results provide some indication of possible spatial priorities under climate change, and so may prove important in helping to generate conservation hypothesis that can be further tested.

Traditional approaches to conservation are often less effective under climate change, due to potential shifts in species ranges. Mediterranean climates such as California are particularly vulnerable because of their large numbers of endemic and threatened species (Midgley et al. 2002). Conservation planning under climate change faces the difficult problem that suitable climate space for species shifts through time, while species' abilities to disperse may not be compatible with the velocity of shifting climates on the landscape (Loarie et al. 2009). Additionally, traditional conservation instruments ranging from strict reserves to conservation easements are static and are likely not positioned with changing climate in mind (Hannah 2005).

Researchers have begun to examine how best to adapt resource management and conservation planning to projected climate change. This section explores the application of a Network Flow Analysis (NFA) as a means of addressing this problem.

The NFA grows out of work on connectivity and climate change that resulted in new methods for prioritizing protected areas (Hannah et al. 2007) and connectivity (Williams et al. 2005). The connectivity approach is valid for identifying areas of connectivity on the periphery of existing protected areas or outside protected areas (for instance, through easements). Williams et al. 2005 used projections of suitable habitat in ten-year time steps to identify "chains" of habitat connected in time. A simple illustration of a connectivity chains through three time steps is shown in Figure 2.1. A heuristic algorithm then selects areas to form chains of suitable habitat that meet a minimum suitable area target across a large number of species with minimum land area.

Phillips et al. (2008) recognized that objective of Williams et al. 2005 could be posed as a general class of problem known as integer programming, which is quite well studied in the computer science community and for which there are a number of highly optimized and efficient

algorithms and software tools. Phillips et al. (2008) used integer programming software to solve the connectivity of suitable habitat through time as a network flow problem. This refined Williams et al. 2005 approach in that it was designed to provide a true optimal value (a more efficient solution in terms of additional protection required for the same conservation benefit), but at the cost of computational complexity and time (and a corresponding difficulty in applying the approach to large spatial domains). The NFA presented here is modeled after Phillips et al. 2008, but conducted with a widely available optimization software package, Gurobi Optimizer version 4.5 (Gurobi 2011).

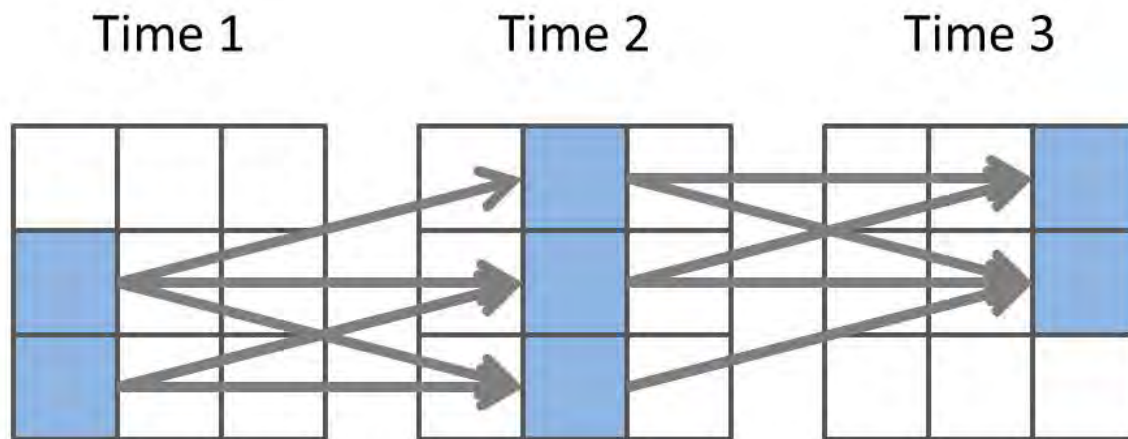


Figure 2.1: Illustration of Chains of Suitable Habitat. Regions shaded blue represent suitable habitat in each time step on a 3 x 3 grid. Grey arrows represent possible chains within a species dispersal capability necessary to retain suitable habitat in all time steps.

The NFA optimizes spatial sharing of connected conservation parcels required to meet a specified minimum conserved area for all modeled plant species over the analytical time period. The resultant outputs represent the specific areas required to ensure spatial and temporal connectivity of suitable habitat through time, constrained by assumptions of a species ability to disperse. Essential connectivity chains identified by NFA that are not currently within either protected areas or developed lands represent potential focal areas for conservation action to adapt the state's conservation portfolio to projected climate change.

2.2 Methods

To identify priority areas for the conservation that can accommodate shifting climatic suitability of native California plant species under climate change, we adapted the NFA of Phillips et al. (2008). In this approach, the modeled range of a single species through time is treated as a directed network, with nodes representing pixels of suitable habitat and edges connecting nodes at one time step with nodes in the next time step that are within a defined dispersal range. A connectivity chain is formed by a continuous path or a set of pixels in which a species can disperse from currently suitable habitat through all time steps to future suitable habitat.

Despite guidance from previous work on this topic, the scope of the problem we set out to solve is large and complex, and so we took several approaches to making the problem tractable. First, we conducted our analysis with modeled ranges of 2,235 native California plant species at

~4 km grid cell resolution (see Section 1 for detailed methods). This relatively coarse resolution was necessary to solve the problem for all species over the statewide domain within a reasonable timeframe to test and refine the methodology. Second, we pre-screened and excluded all species that were able to satisfy their required number of chains using existing protected areas alone. Third, we iteratively performed multiple optimizations, beginning with a few rare species, and gradually added more common species, checking at each step which species satisfied their requirements with the current solution and included only those that did not. Finally, we terminated the optimizations early, such that our solutions were not guaranteed to be globally optimal, but were within some quantifiable error from the true global optimum.

We utilized species distribution maps at decadal time steps based on two climate model outputs (PCM and GFDL under the A2 emissions scenario), two time periods (2000–2050 and 2000–2080), two minimum areas of suitable habitat requirements for all species in each time step (100 and 1000 square kilometers [km²]), and three dispersal radii (0, 6.3, and 10.5 km/time step). The 100 km² target is an International Union for Conservation of Nature (IUCN) threshold for species endangerment. The 1,000 km² target is an arbitrary order-of-magnitude increase in that target and is useful for visualization of important regions for statewide temporal connectivity. The three dispersal assumptions that were modeled included no dispersal, limited dispersal of 1.5 grid cells (the 8-neighbor rule), and intermediate dispersal of 2.5 grid cells (the 25-neighbor rule). Dispersal assumptions were universally applied across all species in a scenario.

Distribution models for native species (as designated by Calflora 2009) with >10 pixels containing known occurrences were generated for each decadal time step in Maxent. Pixels that were classified as developed in the National Land Cover Dataset 2001 (Homer et al. 2004) were considered as never suitable for any species, and were thus excluded from forming chains of suitability in this analysis. We defined existing protected areas as pixels comprising more than two-thirds of protected areas with a GAP³ status of 1 or 2, in either the Conservation Biology Institute or the USGS version of the Protected Areas Database (CBI 2010; USGS 2011). These existing protection pixels are considered protected in perpetuity (i.e., chains can use these pixels without increasing the number of additional protected pixels needed).

To identify potential priority areas for temporal connectivity, we employed two methods. First we highlighted pixels that were selected for additional protection under both the 100 km² and the 1,000 km² suitable habitat requirements (see Figures 2.4 through 2.7). Second, we identified chains that were essential to the solution across all model scenarios (see Figures 2.8 and 2.9).

2.3 Results

Nearly 70 percent of modeled species were able to form connectivity chains within existing protected areas. Additionally, 5 to 10 percent of species (depending on GCM and dispersal assumption) were not able to form the minimum required number of chains. As expected, greater assumed dispersal distance resulted in fewer species that were not able to attain suitable habitat requirements in all time steps (Figure 2.2). Additionally, models with PCM climate data, which shows less dramatic temperature increases and greater precipitation than GFDL within California, allows for more species to attain suitable habitat requirements (Figure 2.3).

³ U.S. Geological Survey, Gap Analysis Program (GAP).

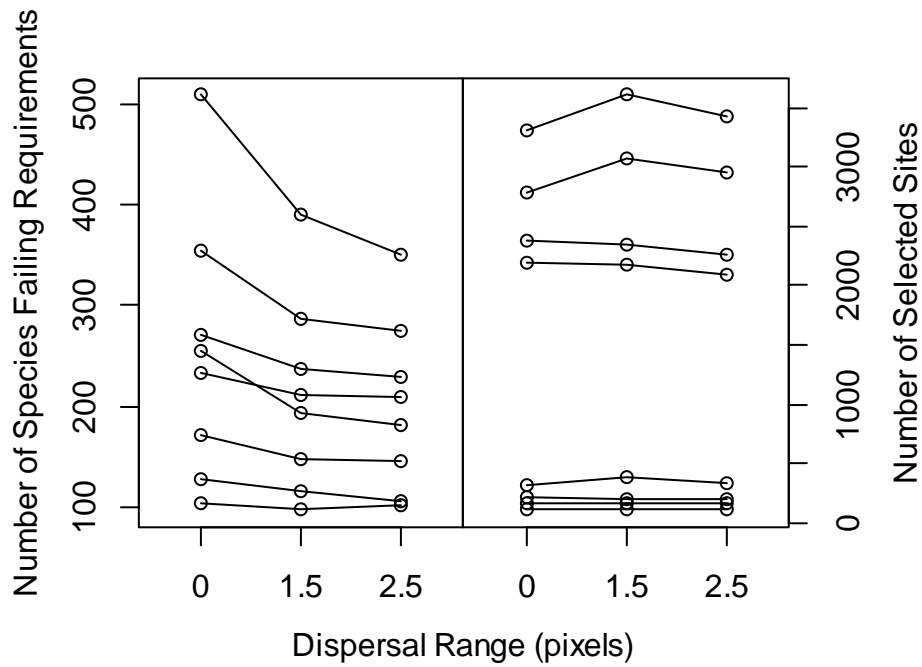


Figure 2.2: Number of Species That Fail Suitable Habitat Requirements (Left Panel) and Total Sites Selected for Additional Protection (Right Panel) by Dispersal Distance Assumption. Each series represents a GCM (PCM or GFDL), time period (through 2050 or 2080), and suitable habitat requirement (100 km² or 1,000 km²) combination.

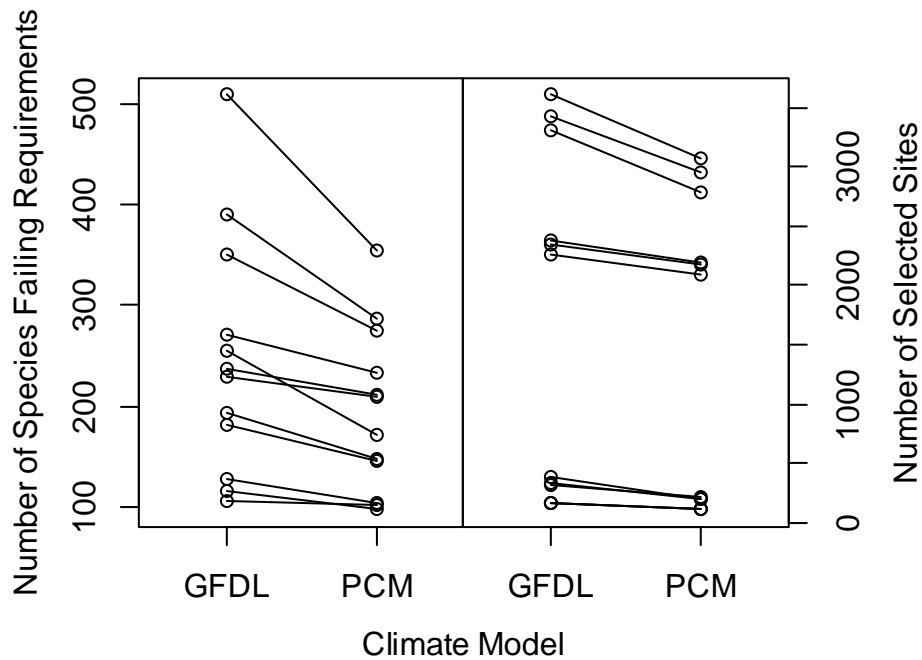


Figure 2.3: Number of Species That Fail Suitable Habitat Requirements (Left Panel) and Total Sites Selected for Additional Protection (Right Panel) by GCM. Each series represents a dispersal assumption (0, 1.5, or 2.5 pixels), time period (through 2050 or 2080), and suitable habitat requirement (100 km² or 1,000 km²) combination.

Species that are able to form chains and meet the suitable habitat requirement in areas that are outside of existing protection account for the “additional protection needed” results. The Figures 2.3 through 2.7 below represent the NFA results under different GCMs and model timeframes. All scenarios presented are for 2.5 cell dispersal per time step and A2 emissions scenario. In each figure, two targets for connectivity are represented, 1,000 km² (57 chains) and 100 km² (6 chains). A majority of the pixels selected for the 100 km² solution are also included in the 1,000km² solution. Such pixels selected for both solutions are shown in red. In the rare case a pixel is selected for only the 100 km², it is shown in magenta. Due to the small total number of 100 km², it may be difficult to distinguish in the statewide views shown below.

Broad areas in several parts of the state are highlighted in yellow and pink, indicating that they are conservation priorities to maintain connectivity for plants as climate changes. Many of these areas are adjacent to existing protected areas, as the algorithm preferentially selects areas that can make use of connectivity within existing protected areas. Land tenure in these priority areas may be private or public. On public multiple-use lands, zonation for biodiversity protection in these priority areas may be appropriate. Private lands may be conserved with conservation easements or through acquisition.

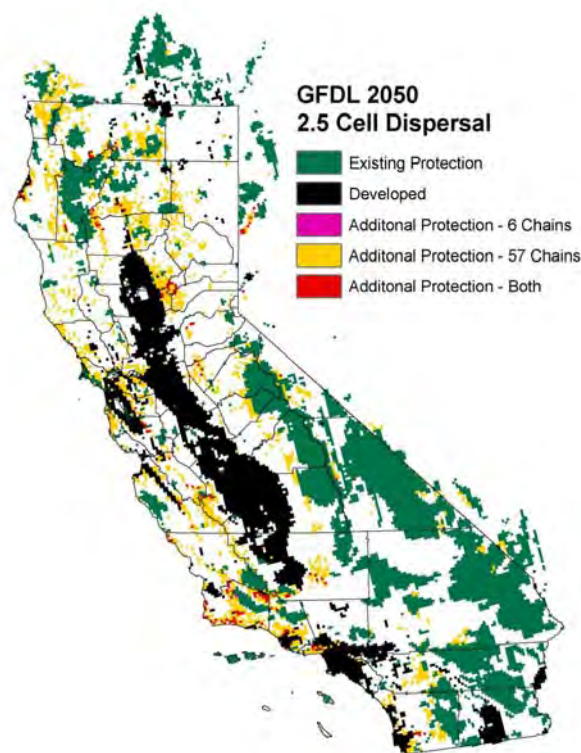


Figure 2.4: Depiction of Areas Required to Form Chains of Protection through 2050 – GFDL, A2 Emissions Scenario; 2.5 Cell/Decade Dispersal Assumption

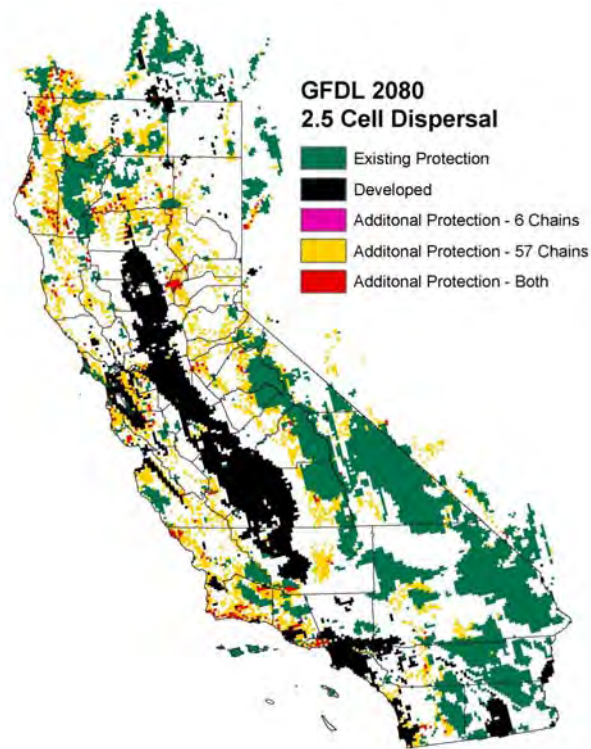


Figure 2.5: Depiction of Areas Required to Form Chains of Protection through 2080 – GFDL, A2 Emissions Scenario; 2.5 Cell/Decade Dispersal Assumption

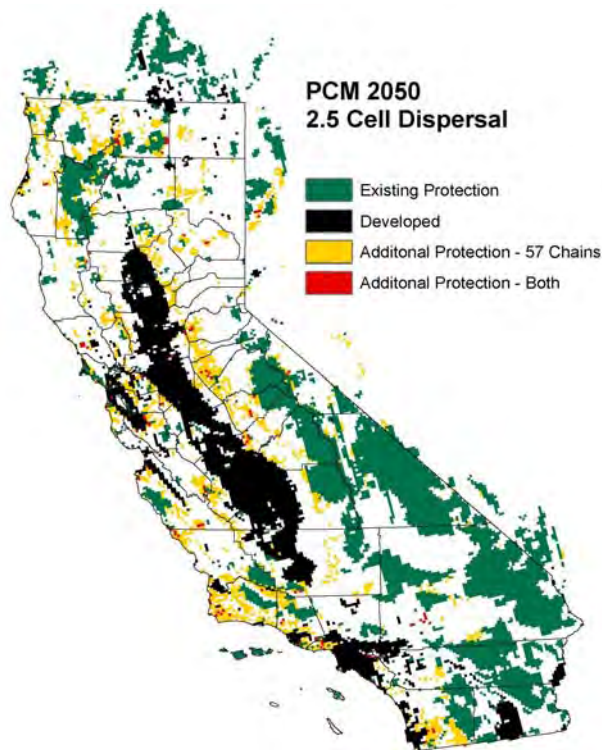


Figure 2.6: Depiction of Areas Required to Form Chains of Protection through 2050 – PCM, A2 Emissions Scenario; 2.5 Cell/Decade Dispersal Assumption

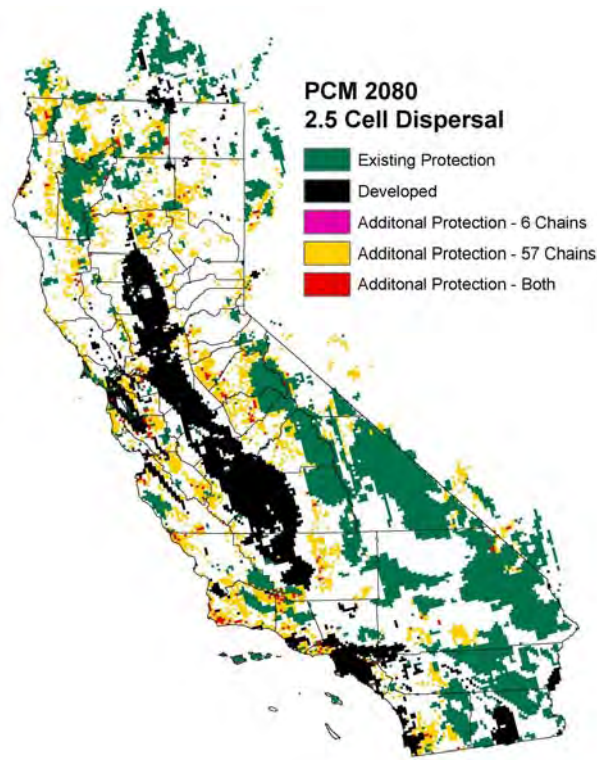


Figure 2.7: Depiction of Areas Required to Form Chains of Protection through 2080 – PCM, A2 Emissions Scenario; 2.5 Cell/Decade Dispersal Assumption

Specific pixels selected for additional protection varied according to GCM and dispersal assumption, but certain regions were consistently selected in each simulation. Stacking the chains required to meet the minimum area target for all species in all model simulations reveals focal areas that deserve consideration for future conservation.

Not all species are able to achieve enough chains to meet the suitable habitat target. The areas which do harbor these species in all time steps represent potential core areas of temporal connectivity. These select areas tend to nest within the yellow 1,000 km² (57 chain) priorities. Chains formed by these species are represented in Figure 2.8. They are “required chains” in the sense that because the species fails to meet the habitat suitability target, anywhere the species *does* have a chain is required in the conservation solution. The NFA outputs may be queried to identify species that are contributing to clusters of “required chains”. This analysis can therefore help to establish species priorities that are linked to spatial priorities. This is illustrated in Figure 2.9, in which several of the “required chains” rare and/or vulnerable species areas are identified. The accompanying Table 2.1 then lists the species that form the required chains within these illustrative areas. The NFA output can be queried to establish species lists for any defined focal areas or to show the chains formed by individual species. As an example, Figure 2.9 depicts the required chains of Purple Sage (*Salvia leucophylla*), which are modeled to be concentrated in Santa Barbara and Ventura counties.

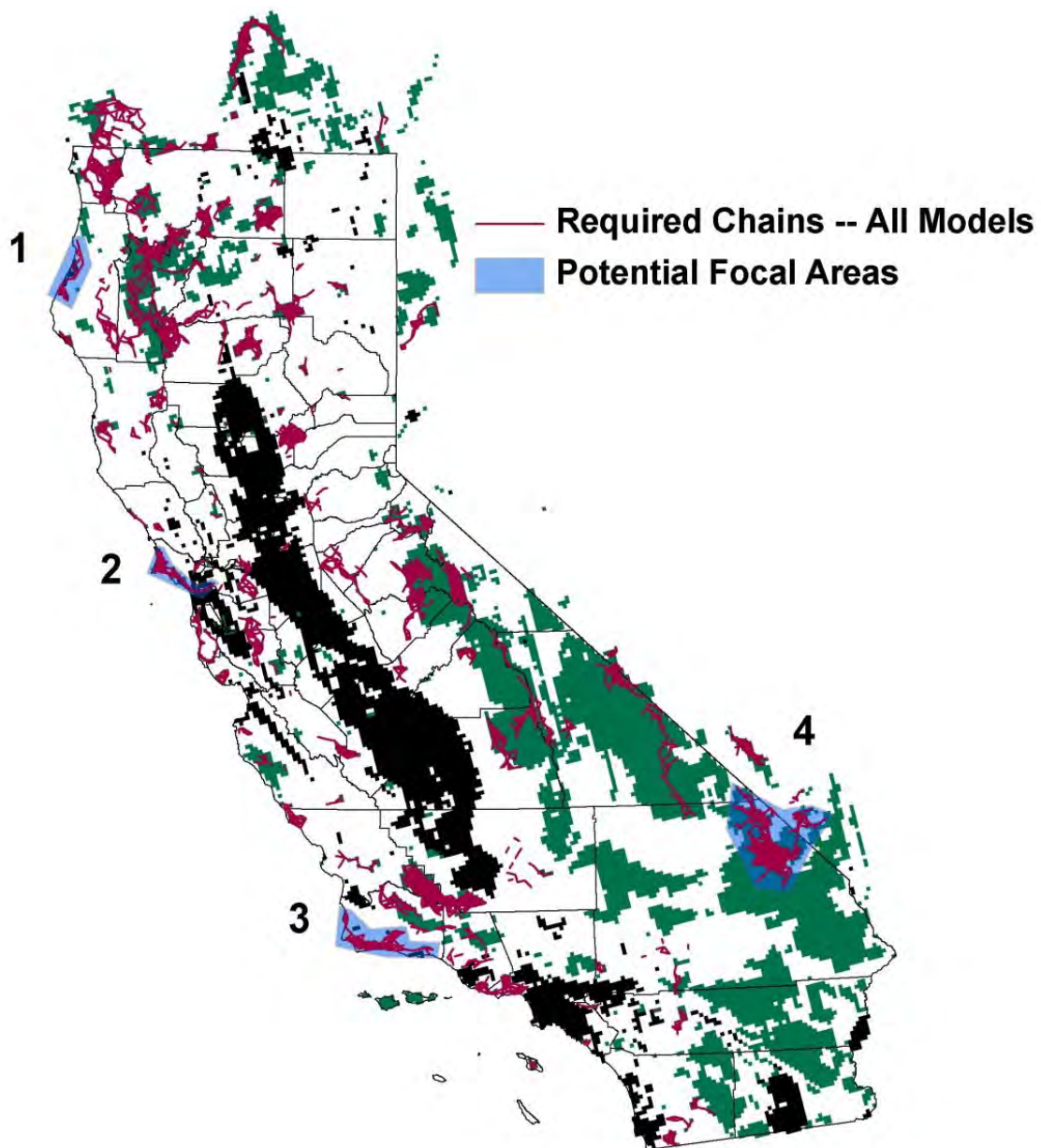


Figure 2.8: Illustrative Focal Areas for Climate Change Connectivity. Regions in blue are polygons enclosing clusters of connectivity chains presented in Figure 2.8. Lists of species responsible for the required chains in each focal area are presented in Table 2.1.

Table 2.1: List of Species Contributing to Required Chains in Illustrative Focal Areas

Focal Area 1	Focal Area 2	Focal Area 3	Focal Area 4
<i>Corylus cornuta</i>	<i>Calamagrostis nutkaensis</i>	<i>Ambrosia chamissonis</i>	<i>Bouteloua eriopoda</i>
<i>Cyperus eragrostis</i>	<i>Calystegia subacaulis subacaulis</i>	<i>Atriplex lentiformis</i>	<i>Brickellia desertorum</i>
<i>Euthamia occidentalis</i>	<i>Campanula californica</i>	<i>Calochortus catalinae</i>	<i>Mirabilis multiflora</i>
<i>Helenium puberulum</i>	<i>Cardionema ramosissimum</i>	<i>Ceanothus megacarpus</i>	<i>Muhlenbergia porteri</i>
<i>Salix lucida</i>	<i>Cirsium brevistylum</i>	<i>Ceanothus spinosus</i>	<i>Pleurocoronis pluriseta</i>
<i>Satureja douglasii</i>	<i>Cirsium quercetorum</i>	<i>Chaenactis glabriuscula orcuttiana</i>	
	<i>Grindelia stricta</i>	<i>Chorizanthe breweri</i>	
	<i>Helenium puberulum</i>	<i>Encelia californica</i>	
	<i>Lotus wrangelianus</i>	<i>Eriogonum crocatum</i>	
	<i>Lupinus arboreus</i>	<i>Lepechinia fragrans</i>	
	<i>Lupinus chamissonis</i>	<i>Lomatium lucidum</i>	
	<i>Potentilla anserina</i>	<i>Lupinus longifolius</i>	
	<i>Ribes menziesii</i>	<i>Opuntia littoralis</i>	
	<i>Trifolium willdenovii</i>	<i>Opuntia oricola</i>	
		<i>Oxalis albicans</i>	
		<i>Populus fremontii</i>	
		<i>Salvia leucophylla</i>	
		<i>Sanicula arguta</i>	
		<i>Typha latifolia</i>	
		<i>Venegasia carpesioides</i>	
		<i>Viola pedunculata</i>	

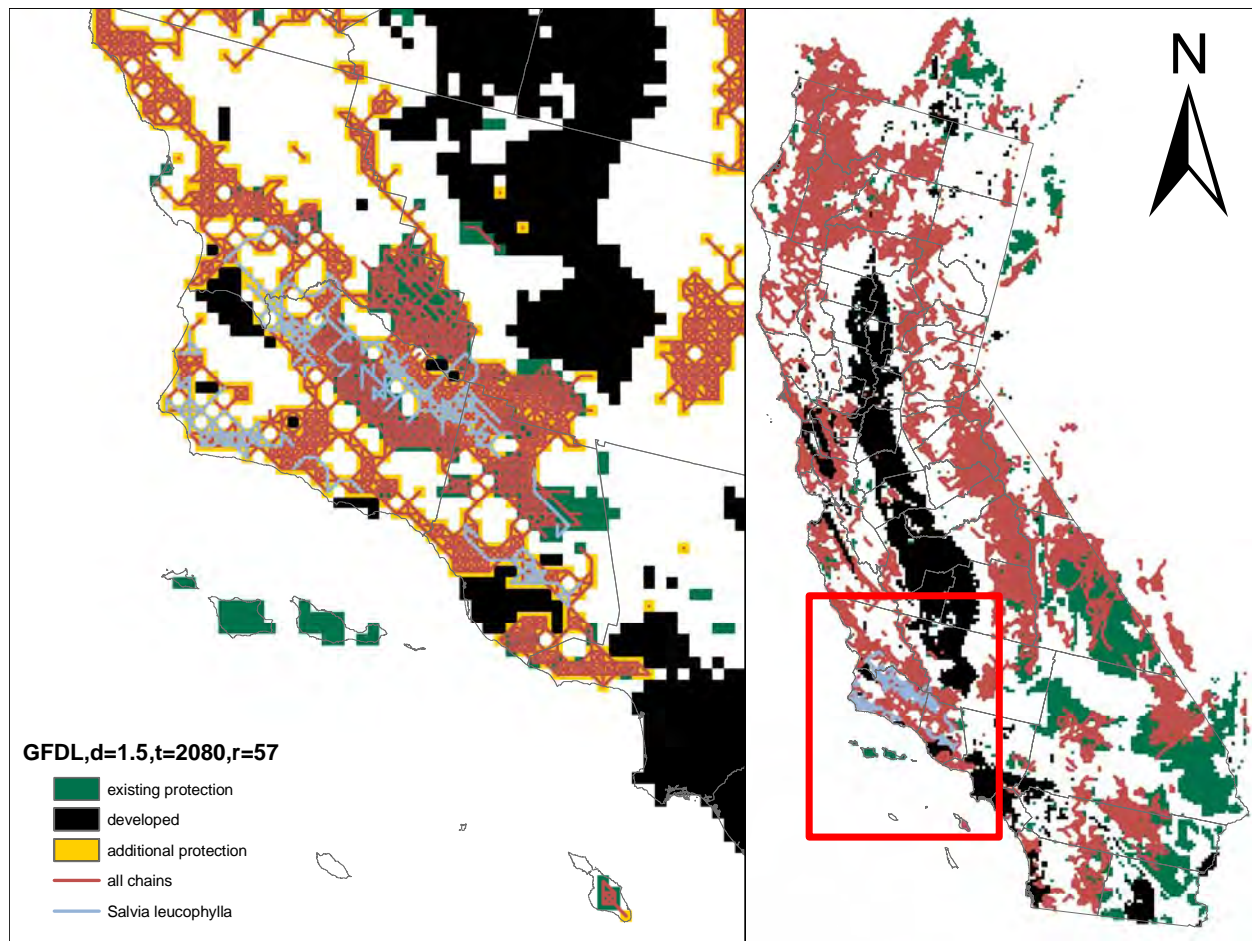


Figure 2.9: Required Chains of *Salvia Leucophylla* (Blue) Overlaid on All Connectivity Chains Formed Under GFDL Climate Projections Through 2080. Model outputs shown assume 1.5 pixel dispersal distance and 1,000km² suitable habitat (57 chains) requirement.

2.4 Discussion

The results presented in this paper represent a successful demonstration of NFA to address the problem of spatio-temporal connectivity of suitable habitat under climate change for a large number of species and a spatial domain the size of California. Successful testing and implementation of the methodology involved several simplifying assumptions that contribute to limitations of these demonstration results. As described earlier, relatively coarse grid sizes (~4 km) were required to optimize the solution for the entire species dataset at a statewide modeling domain. Habitat suitability models at this resolution may not accurately account for topo-climatic processes that control suitability at biologically relevant scales, and therefore may miss pockets of suitability (i.e., micro-refugia) that may exist within a fractional portion of a ~4 km grid cell. The effect conducting NFA at this scale is potentially a greater issue for narrowly distributed species or habitat specialists (e.g., riparian species). Additionally, although the habitat suitability models are constructed with soil parameters as a predictor variable (see methods in Section 1), the variability of soils within a grid cell will not be captured at this resolution. This may lead to spurious results for species whose distributions are governed by specific soil requirements such as serpentine specialists. The implementation of NFA at finer

resolutions over smaller spatial domains and/or shortened species lists is an important next step in the refinement and applicability of the methodology.

The universal assumption of a constant dispersal rate for all species is another major qualification of the results of this demonstration. Clearly, species vary in their capacity to disperse – and viable dispersal distances for an individual species will vary in different landscapes. Variable life history among species represents additional modeling challenges. Slow-to-mature species may not be able to produce reproductive offspring within the decadal time step, therefore limiting a species to keep pace with shifting suitability even if suitable habitat is within measured dispersal distances for mature adults. Similarly, for long-lived species, the pixels they occupy may become unsuitable for recruitment but retain reproducing and dispersing mature individuals. Inclusion of variable dispersal distances or time step frequency within the NFA algorithm is not infeasible, but will likely require abbreviated species lists and regional focus. These refinements to the model initialization are research priorities moving forward.

2.5 Conclusions

The NFA has been successfully demonstrated as a viable means for optimizing spatio-temporal connectivity for large groups of species in California. Unprotected areas that are identified by NFA potentially represent important areas for the adaptation of statewide conservation strategy to climate change and such identification will help to ensure continued protection for all species under shifting climates. This initial demonstration has several limitations, including relatively coarse grid size and universal dispersal assumptions, but ongoing refinements to the methodology point to a promising tool to evaluate connectivity of shifting California species ranges in a changing climate.

Section 3: Impacts on Plant Communities of Changes in Viticulture

3.1 Introduction

3.1.1 Background

Conservationists are increasingly aware that there are both direct and indirect impacts of climate change on natural systems. The last two decades of study have focused on the direct impacts on species and ecosystems (reviewed by Heller and Zavaleta 2009 and Mawdsley et al. 2009). Recent literature has begun to focus on indirect impacts due to human translocation and shifts in agriculture due to climate change (Turner et al. 2010). To capture first insights into indirect impacts on conservation, this study chose one agricultural commodity to assess for the impacts that climate-driven change in agriculture might have on ecosystems. The commodity we chose to focus on is grapes grown for wine production, which is famously sensitive to climate change, as well as being an industry with a history of environmental awareness and stewardship. Here we focus on viticulture in California, a state which accounts for over 90 percent of U.S. wine production and is the fourth largest wine producer in the world behind France, Italy, and Spain.

Global context is as important as local impact, as we have learned in previous assessments of climate change impact, such as the soon-to-be-published analysis of climate change impacts on timberlands in California (Hannah et al. 2011). Climate change-driven global production changes can alter prices in ways that can overwhelm local changes in production. For this reason, we have conducted both global and statewide assessment of changes in viticulture suitability and the possible resultant consequences for conservation.

The practice of premium viticulture has long been tied to an ideal combination of climate, geography, and culture often referred to as *terroir* (Vaudour 2002). The world's most famous wine grape growing regions are romanticized for the climatic attributes that contribute to each region's particular style of wine produced, as well as for the assemblage of varieties that thrive in the setting. Individual vintages are heralded as the precise combination and timing of climatic events within a particular growing season. Furthermore, there is evidence that the spatial distribution of viticulture has tracked broad trend in global climate; shifting northward during the Medieval warm period of the thirteenth and fourteenth centuries and retracting to the south during subsequent cooler period leading up to the Little Ice Age of the nineteenth century (Pfister 1988). Establishment of major viticulture areas outside of continental Europe has primarily occurred in locations that mimic the climates of proven European areas of production. As a result, areas with Mediterranean climate regimes such as Chile, South Africa, Australia, and California have emerged as globally significant sources of viticulture for premium wine production. Given the importance of climate in determining the global distribution of wine grape growing regions and the sensitivity of wine quality to the local-scale climate events of a given growing season, it is anticipated that twenty-first century climate change will have an appreciable impact on the wine industry within California and worldwide.

3.1.2 Previous Work Linking Climate to Viticulture

Several previous research efforts have laid the groundwork for establishing the link between climate and suitability for viticulture. Seminal publications such as Winkler et al.'s *General*

Viticulture (1974) and Gladstones' *Viticulture and Environment* (1992), as well as his newly released *Wine, Terroir and Climate Change* (2011) have extensively characterized the climatic and geomorphological settings of global wine grape growing regions. These publications emphasize mean annual temperature and annual heat summation (as measured by mean daily temperature above a defined threshold) as principal determinants of general viticulture suitability, as well as optimal varietal composition for a given region. Several subsequent studies have built on this work to assess viticulture suitability in terms of mean annual temperature and heat summation under climate change (e.g., Nemani et al. 2002; Jones et al. 2005; Hayhoe et al. 2004; White et al. 2006).

In addition to long-term average climate, other studies have examined the impact of the changing frequency of extreme events (heat or cold) on long-term viability of viticulture under climate change (e.g., White et al. 2006; Diffenbaugh et al. 2011). Yet others have fine-tuned suitability models to link the effects that yearly climate has on yields (Lobell et al. 2007) or quality (Jones et al. 2005; Nemani et al. 2002) of wine produced in a given location. For California, a majority of recent studies project a redistribution of optimal viticulture climate in the coming decades that will likely engender adaptive responses from the viticulture industry.

3.1.3 Novel Aspects of this Study

This study takes advantage of newly produced fine-scale climate data to model optimal climates for viticulture within California at 270 m horizontal resolution. Modeling at this resolution will better capture local-scale processes that help to control climatic suitability. The model results presented in this section are the consensus among three previously published methods used to determine viticulture suitability. A viticulture occurrence dataset (see Methods) that samples California vineyard locations on the basis of American Viticulture Area (AVA) boundaries was produced for this study to correlate existing climate conditions with vineyard locations. This study was conducted in parallel with a larger effort that models global viticulture suitability. This allows us to place the climate change impacts on California viticulture in context with what is happening on a global scale. Finally, this study assesses the potential intersection of shifting viticulture climates with land and freshwater conservation interests in California, representing the first such statewide analysis.

3.2 Methods

3.2.1 Viticulture Suitability Models

We used three viticulture suitability models, representing each of three broad classes of suitability models that have been proposed based on (1) average or extreme growing season temperatures, (2) phenology, and (3) multiple variables. For the temperature approach, we chose average temperature during the growing season—the most commonly applied temperature model. From the phenological approaches previously published, we selected growing degree day accumulation, the most often utilized of this category. We used Maxent, a widely used climate-distribution model (also known as species distribution model, niche model, or bioclimatic envelope model) to represent multiple variable models, because of its broad acceptance and ease of application. Our implementation of each of these three models is described below.

3.2.1.1 Temperature - Average Growing Season Temperature

Optimal average growing season temperatures for twenty-one common varieties of wine-producing *V. vinifera* were approximated from global distributions and viticulture regional climates in Jones et al. 2005. Taken together, the optimal range for common wine varieties spans average growing-season temperatures from 13.1°C–20.9°C (55.6°F–69.6°F). In modeling current and projected suitability with average growing season, areas falling within this optimal range were considered suitable. Growing season was defined as April 1–October 31 in the Northern Hemisphere and October 1–April 30 for the Southern Hemisphere.

3.2.1.2 Phenology – Growing Degree Day Maturity Groupings

The phenological method is adapted from Hayhoe et al. (2004), in which viticulture suitability in California is determined by biophysical response of grapevines as ripening progresses. Gladstones (1992), assembled common wine grape varieties into eight distinct maturity groupings, depending on the heat summation required for fruit maturity and ripening. The timing of ripening for each grouping is determined by summing the biologically active growing degree days (GDD) above 10°C (50°F). For example, cooler weather varieties such as Pinot Gris require 1,100 GDD for ripening; whereas, Grenache ripens after 1,350 accumulated GDD. In this analysis, the month in which the required GDD summation is reached is used to determine suitability for viticulture. Average ripening month temperatures in the range 15°C–22°C (59°F–72°F) are considered optimal, 22°C–24°C (59°F–75°F) is marginal and > 24°C (> 75°F) impaired (after Gladstones 1992; Hayhoe et al. 2004). A location was deemed suitable for viticulture if average ripening month temperature is optimal for any of the eight maturity groupings.

3.2.1.3 Multiple Variables - Maxent

The Maxent climate-distribution model takes as input a set of layers or environmental variables (e.g., elevation, precipitation), as well as a set of occurrence locations, and produces a model of climatic suitability for a species. We used this approach to model suitable climate space for cultivation of *V. Vinifera*. The bioclimatic predictor variables used in Maxent modeling were:

- Average temperature in growing season
- Total precipitation in growing season
- Precipitation seasonality (C of V)
- Total GDD in growing season
- Mean maximum temperature of the warmest month during growing season
- Mean minimum temperature of the coldest month during growing season
- Mean diurnal range (mean monthly max-min)
- Mean minimum temperature of the coldest month
- Annual precipitation
- Aridity Index (annual precipitation/potential evapotranspiration)

3.2.1.4 Minimum Temperature and Precipitation Constraints

At the northern boundaries of wine-growing regions, chilling stress during growing season and overwinter minimum temperatures are limiting factors in determining viticulture suitability. Overwinter cold hardiness of *V. vinifera* varies according to age of the vine, varietal, and seasonal timing of annual minimum temperatures. However, temperatures below -12°C (10°F) begin to impart tissue damage that can impair production, and temperatures below -25°C (-13°F) are lethal to most varieties. To create a conservative threshold for excess risk of frost

damage, areas with mean minimum temperature of the coldest month $< -15^{\circ}\text{C}$ ($< 5^{\circ}\text{F}$) were classified as unsuitable for viticulture.

Too much or too little precipitation can make a region unsuitable for growing high-quality wine grapes. We compiled annual precipitation data for global wine regions ($n = 135$) from Gladstones 1992 and Johnson and Robinson 2007. We assumed mean annual precipitation of these regions plus or minus two standard deviations as upper and lower bounds of annual precipitation in determining wine-growing suitability. As such, areas with $> 1,226$ mm and < 200 mm of precipitation were used as constraints defining areas as unsuitable for viticulture.

Minimum temperature and precipitation constraints were applied to the average temperature and phenology models. The constraints were not applied to Maxent multifactor modeling results, as minimum annual temperature and annual precipitation were included as predictor variables.

3.2.2 Climate Data

3.2.2.1 California Modeling

Climate data used to model the distribution of viticulture climates within the State of California was the same downscaled climatology used to produce the 270 m species distribution models described in Section 1. In all cases, viticulture suitability models in California were built on 30-year averages of the relevant bioclimatic parameter. Viticulture suitability was modeled for current climate and future climates covering the time periods 2040–2070 and 2070–2100. For the California domain, GFDL and PCM projections were modeled individually.

3.2.2.2 Global Modeling

Current climate (mean monthly maximum temperature of the warmest month, mean minimum temperature of the coldest month, and total precipitation on a 30-year average) and elevation data (derived from DEM) on 2.5 arc minute grids (approximately 5 km) were downloaded from the Worldclim website (<http://www.worldclim.org>). Data were originally downloaded on March 29, 2010 (Hijmans et al. 2005).

Future global climatologies representing twenty-year normals for the time periods 2041–2060 and 2081–2100 were downscaled from five general circulation models to a 2.5 arc minute grid, as described by Tabor and Williams 2010. The GCMs used in the global analysis were:

- CCSR/NIES/FRCGC, Japan, MIROC3.2, medium resolution
- CSIRO Atmospheric Research, Australia, Mk3.5 Model
- Bjerknes Centre for Climate Research, Norway, BCM2.0 Model
- National Center for Atmospheric Research, United States, CCSM3.0
- Institute for Numerical Mathematics, Russia, INMCM3.0 Model

The globally downscaled climate data were obtained from the Conservation International climate data portal (<http://futureclimates.conservation.org/index.html>).

To limit the uncertainty introduced by the projections of an individual GCM, we modeled suitability as an ensemble average of the five GCMs for each climate/emissions scenario and suitability model. Viticulture suitability in each scenario was defined as consensus agreement among all three suitability models.

3.2.3 Viticulture Occurrence Points

3.2.3.1 *California Modeling*

A dataset of occurrence points for viticulture within California was built for the multifactor Maxent modeling component of this analysis. Occurrence points in the dataset ($n = 225$) represent a quasi-random sampling of vineyards within California American Viticulture Areas (AVAs) that were visually identifiable in 2010 satellite imagery as accessed through Google Earth. Active viticulture at an occurrence point was verified by publicly available information regarding the nearest vineyard or winery, as indicated by a Google Maps search of each candidate occurrence point. Vineyards were selected for the dataset so as to represent the geographic extent and topographical diversity of each primary AVA. The strategy of surveying vineyards within each AVA was used to focus the search for visually identifiable vineyards. Also, as AVAs are established by vintner petition partly on the premise of distinct growing conditions, this strategy captures the full range of climates and soil types currently under vine in California. As petitioning for the designation of an AVA may be motivated by marketing strategy and/or product differentiation, AVAs—and thus occurrence points—are in greater density within regions internationally recognized for consistently producing high-quality wines. The density of occurrence points therefore does not necessarily correlate with county statistics of vineyard acreage (NASS 2010), and prolific grape-producing counties in the comparatively large Central Valley AVA are not as well represented as the more topographically diverse Napa, Sonoma, and Mendocino counties.

3.2.3.2 *Global Modeling*

Occurrence points ($n = 1129$) for viticulture were taken from a geo-referenced global dataset. Location points within the dataset were established primarily from publicly available national viticulture jurisdiction boundaries, supplemented with expert input from the wine industry where this information was unavailable or not able to be verified.

3.2.4 Protected Area Mask

Protected area locations and extents are taken from the 2011 California Protected Area Database (CPAD 2011). Polygons of the CPAD were converted to match the 270 m grid cell size of the viticulture suitability layers. A grid cell was classified as “protected” if > 50 percent intersected with a protected area polygon. Protected areas of all IUCN categories I–VI were then masked out of the viticulture suitability maps for both current and future climates, under the assumption that viticulture will continue to be an excluded activity on protected lands. All results presented here have omitted any current or future climatic suitability that occurs with existing protected areas.

3.2.5 Soils and Topography

In addition to climate, a suitable growing substrate is essential for premium viticulture. The specific mineral make-up, nutrient content, depth, and water-holding capacity of a particular vineyard’s soil profile are important variables in the health and productivity of the resident vines. Vineyard-scale variation in soil attributes may dramatically affect the yield and composition of grapes within a vineyard block. As the favored style of a particular vintner may command specific soil requirements, local soil composition is indeed an important variable in vineyard siting decisions. However, the specific soil requirements of high quality wine are often over-emphasized, as evidenced by the fact that premium wines are produced from a broad

spectrum of soil types. The overarching influence of climate is succinctly articulated in Winkler et al.'s *General Viticulture*

“Even in the renowned wine-producing areas of Europe, with their varied soils, heat summation must be accepted as the principal factor in the control of quality: their vintage years always coincide with abundance of heat, and such years occur uniformly across all soil types.”

Additionally, ambient soils are often actively managed to compensate for nutrient deficiencies or to strategically stress the vines to enhance sugar content of the grape cluster. As a result, with the exceptions of sufficient rooting depth and toxicity resulting from salinity or ultra-mafic minerals, the limiting factors of soil for viticulture suitability are difficult to generalize.

To account for soil type variation within California, we used STATSGO2 data for soil parameters within the Maxent multifactor modeling. We used a database based on soil types to generate low-level available water capacity, pH, and soil depth from http://www.soilinfo.psu.edu/index.cgi?soil_data&conus&data_cov&awc&methods.

Attributes of the soil type polygons were converted to the 270 m resolution of the climate data used in generating suitability models. It should be noted that the soil parameters used in this analysis are uniform within each polygon and that finer scales do not result in greater resolution of fine-scale soil variation. Our modeled suitability results demonstrate where the potential for successful cultivation of *V. vinifera* is likely, due to favorable average climatic conditions and soil type. Specific vineyard siting decisions within each 270 m grid cell and sub-vineyard scale “precision viticulture” management recommendations are important priorities for research into more precise local impacts of climate change.

3.3 Results

3.3.1 Future Projections of Optimal Viticulture Climates within California

3.3.1.1 California Occurrence Points

Applying the suitability models described above, including topo-climate and soil parameters on projections of climate change for mid-century (2040–2070) and end of century (2070–2100) time periods, results in a significant spatial relocation and an overall reduction of optimal viticulture climates within California (Figure 3.1). As with other species models presented in Section 1, the general trend is for viticulture climates to shift northward, coastward, and upslope as mean growing season temperatures increase. The degree of shift varies by GCM projections and emissions scenario, with the comparatively hotter and drier GFDL resulting in a more pronounced shift and steeper decline of optimal climates than PCM projections over the same time period. Likewise, the business-as-usual A2 emissions scenario with unabated emissions has greater impact than the B1 scenario, particularly for end-of-century projections.

The ratio of modeled suitable acreage in future scenarios to current modeled suitability is shown in Table 3.1 for counties with the top currently suitable acreage. Viticulture areas in counties on the eastern and southern edges of the band of modeled current suitability (e.g., Napa, San Benito, Ventura counties) show appreciable declines in total suitable acreage by mid-century and, in some cases, total displacement of optimal climates by end of century. More coastal or northerly counties (e.g., Marin, Mendocino, Monterey) at times show marginal

increase in total suitable acreage by mid-century and less precipitous declines in end-of-century projections.

It is important to view these results as a representation of impacts on viticulture as it is currently practiced and absent any adaptive or mitigation responses available to wine grape growers. Areas that show projected declines of optimal climates for viticulture are best interpreted as areas that will require some adaptive response on the part of wine grape growers or consumers to continue the practice of viticulture in that location. The results are consistent with those presented in White et al. 2006, Diffenbaugh et al. 2011 and Chaplin-Kramer (this paper series 2012) in that total area optimal for viticulture is expected to decline substantially with a shift toward marginal and impaired growing conditions under twenty-first century warming.

It is possible that projected warming may result in short-term gains in either yield or quality for select growing regions, as suggested by Nemani et al. 2001, but the overall redistribution of optimal viticulture climates indicates the necessity of adaptation by the California viticulture industry in the coming decades. Adaptation measures available to wine grape growers include vineyard relocation to more suitable climates, enhanced water development for irrigation or vine cooling, adoption of more heat tolerant varieties, and vine orientation or trellising techniques to manage shading of the grape clusters. The adaptation measures vary in their economic feasibility and barriers to implementation. For a discussion of the relative merits and ease of implementation among adaptation measures, see Diffenbaugh et al. 2011. Adaptation measures that will potentially have the most direct impacts on conservation—the relocation of vineyards to more suitable climates on currently undeveloped land and enhanced water development—will be explored later in this section.

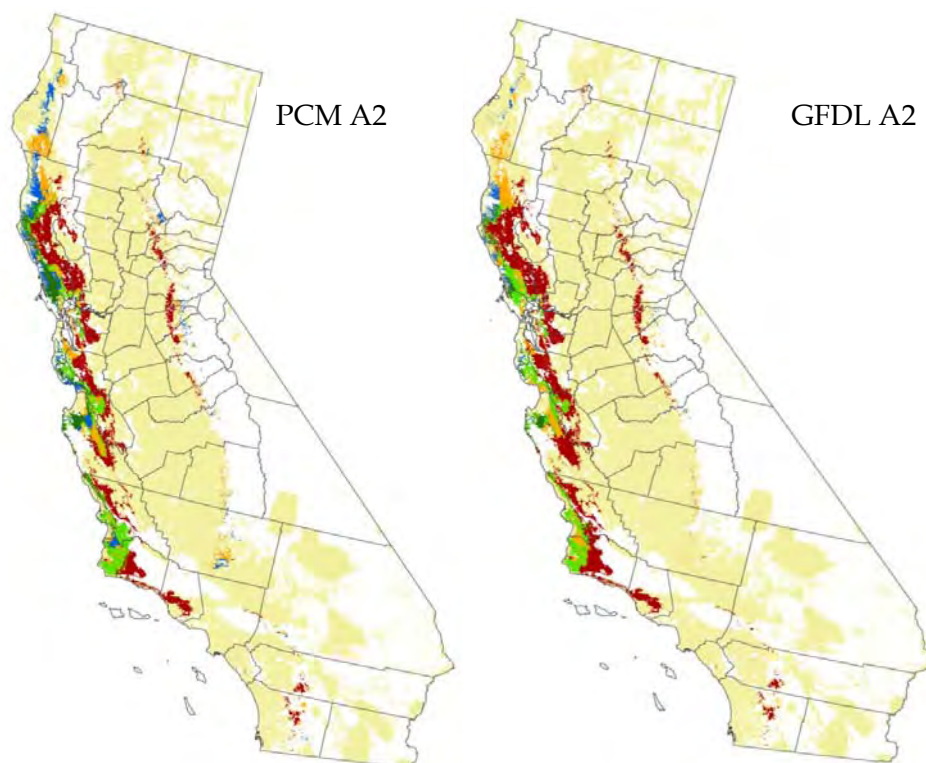


Figure 3.1: Modeled Distributions of Suitable Climates for Viticulture under the A2 Emissions Scenario for Three Time Periods: 1971–2000 (Red); 2040–2070 (Orange); 2070–2100 (Blue). Light Green shows suitability retained through 2070, and Dark Green denotes suitability retained through 2100. Distributions in each time period represent a consensus agreement of three suitability models: (1) mean growing season temperature, (2) maturity grouping heat summation, and (3) Maxent. The Maxent models used in this scenario are built on California viticulture occurrence points and topoclimate + soil predictor variables.

Table 3.1: Change in Climates Currently Associated with Viticulture in California. Negative values of change can be interpreted as the percent of currently suitable land that will require adaptation measures for continued viticulture.

County	GFDL Mid-Century (% change)	GFDL End-Century (% change)	PCM Mid-Century (% change)	PCM End-Century (% change)
Napa – Sonoma – Mendocino	-44	-86	-29	-60
Monterrey – San Luis Obispo – Santa Barbara	-54	-97	-34	-82
California Total	-54	-93	-34	-72

3.3.1.2 Global Viticulture Climates Projected onto California

When the Maxent distribution model constructed with global viticulture occurrence points is projected on California, the broader spectrum of optimal viticulture climates (encompassing both warmer and cooler climates than those associated with existing California viticulture) opens substantially more potentially suitable area than viticulture models built on California occurrence points alone—nearly double the modeled current acreage (Figure 3.2). Declines in total optimal area within California are muted compared to California-only viticulture, and significantly more novel area is projected for northern coastal areas and somewhat unconventional areas of the northern interior (Figure 3.2; Table 3.2).

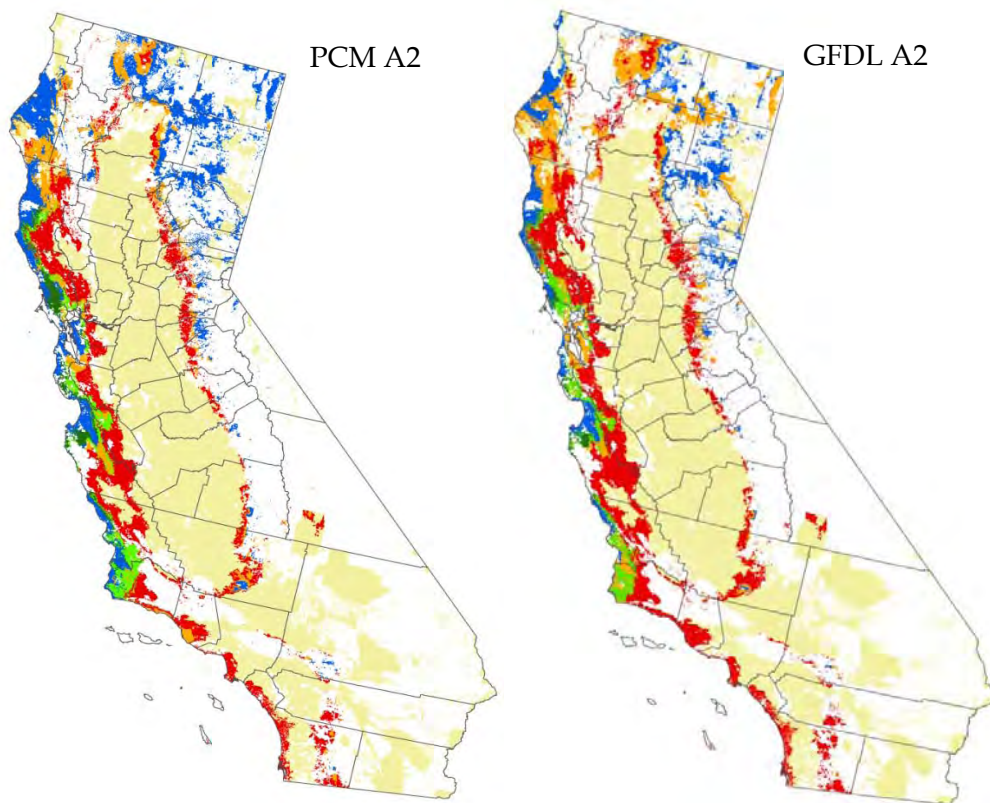


Figure 3.2: Modeled Distributions of Suitable Climates for Viticulture under the A2 Emissions Scenario for Three Time Periods Using Global Viticulture Occurrence Points: 1971–2000 (Red); 2040–2070 (Orange); 2070–2100 (Blue). Light Green shows suitability retained through 2070 and Dark Green denotes suitability retained through 2100. Distributions in each time period represent a consensus agreement of three suitability models: (1) mean growing season temperature, (2) maturity grouping heat summing, and (3) Maxent. The Maxent models used in this scenario are built on global viticulture occurrence points and topoclimate-only predictor variables.

Table 3.2: Change in Climates Currently Associated with Viticulture by County Using Global Viticulture Occurrence Points and A2 Emissions Scenario. Negative values of change can be interpreted as the percent of currently suitable land that will require adaptation measures for continued viticulture.

County	GFDL Mid-Century (% change)	GFDL End-Century (% change)	PCM Mid-Century (% change)	PCM End-Century (% change)
Napa – Sonoma – Mendocino	-42	-78	-33	-59
Monterrey – San Luis Obispo – Santa Barbara	-58	-86	-46	-69
California Total	-32	-69	-23	-45

3.3.2 Global Context

The same processes that will affect viticulture within California under climate change will also affect viticulture worldwide. To fully understand the impact of climate change on California viticulture, it needs to be put into context with what is occurring on a global scale. To place California in the appropriate context, we compare the impact of climate change on California viticulture to those projected in other prominent wine-producing regions. Additionally, we build an alternate model of viticulture suitability within California that incorporates global viticulture occurrence points to better capture the full spectrum of climates where viticulture is currently practiced worldwide.

Figure 3.3 illustrates the projected impacts of climate change on the global distribution of optimal viticulture climates under the A2 emissions scenario. As in California, increasing temperature causes the global patterns of viticulture climates to shift northward, coastward, and upslope of many existing viticulture areas (Figure 3.3). Several high-profile wine grape growing (e.g., Mediterranean Basin, South Africa, Australia) regions show significant loss of existing optimal wine grape growing climates by mid-century and further declines by end of century (Table 3.3). Mediterranean systems are particularly affected, with many losing over 90 percent of existing optimal areas. The translocation of optimal climates opens novel areas of potential viticulture suitability, particularly in northern Europe, interior regions of western North America, and the southern islands of Tasmania and New Zealand. Globally, the loss of existing suitability and the gain of novel suitable areas is almost perfectly balanced by mid century under the A2 scenario. However, by end of century the global stock of climatically optimal area is only 63 percent of total current area.

Although California does experience a significant translocation and decline of existing optimal climates, when the balance of total suitable area is considered, California fares better than all other wine-producing regions in Mediterranean systems (Table 3.3) in both mid-century and end-of-century projections. Also, the ratio of current to future suitable area within California is roughly 20 percent lower than the global total. This is substantially lower, though not catastrophically so, as is the case in other Mediterranean systems. Therefore, although California viticulture will certainly be affected by twenty-first century climate change, the impacts are likely to be muted, as compared to many other major wine-producing regions.

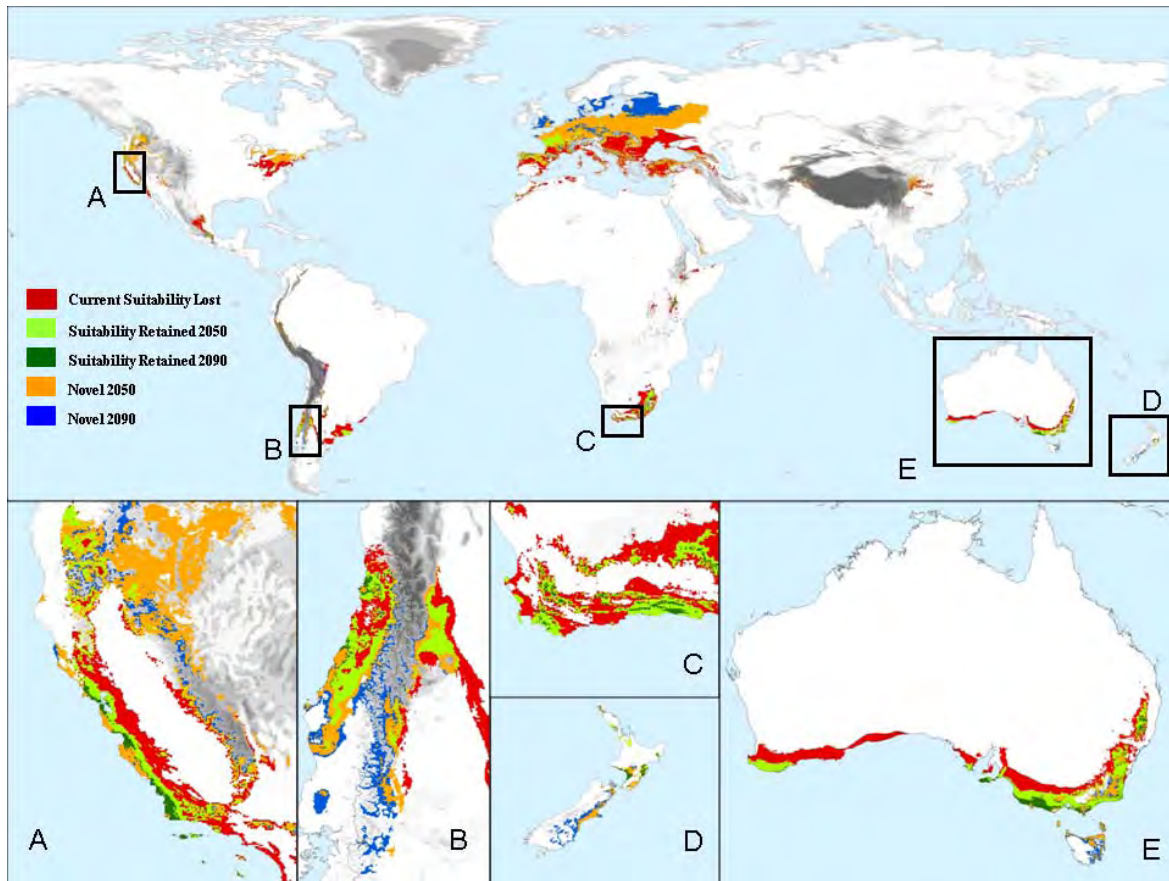


Figure 3.3: Climate Change Impacts on Viticulture Suitability Are Illustrated for Three Time Periods (Present, 2050, and 2090) Based on a Consensus Approach Using Multiple Suitability Models and an Ensemble Projection of Future Climate under the A2 Emissions Scenario (IPCC AR4). Broad areas of current suitability are lost by 2050 in all major wine-producing regions (red). Large areas of new suitability (2050 orange; 2090 blue) open in Northern Europe and North America. Insets A–E show regional detail. Areas where viticulture is retained through mid-century and through all three time periods are shown as light green and dark green, respectively.

Table 3.3: Projected Loss of Currently Suitable Area and the Ratio of Total Future Suitability to Current Suitability in Select Wine-Producing Regions – A2 Emissions Scenario

	% Current Suitability Lost 2050	% Current Suitability Lost 2090	Total Area 2050/Current	Total Area 2090/Current
Globe	73.6	96.1	.995	.628
Mediterranean Systems				
Mediterranean Basin	61.7	92.4	.383	.076
California Floristic Province	60.3	93.1	.744	.469
Central Chile	46.1	95.4	.736	.215
SW Australia	75.5	97.3	.255	.027
Cape (South Africa)	47.8	87.2	.564	.174
Non-Mediterranean Systems				
Northern Europe	90.2	99.6	2.053	1.656
Eastern North America	33.0	99.1	.929	.430
Western North America	64.3	100	17.621	16.366
New Zealand	5.6	45.2	2.417	3.594
SE Australia	48.4	86.7	.626	.261

3.4 Potential Conservation Impacts

Adaptive responses of the viticulture industry that involve vineyard relocation to more suitable climates, expansion into novel areas, or enhanced water development will have potential impacts on terrestrial and freshwater conservation. The conservation impacts are possible both in areas of existing viticulture that experience declining suitability as well as novel areas.

It has been demonstrated that expansion of viticulture over the past two decades has resulted in conversion and fragmentation of oak woodland habitats (Merenlender 2000), the displacement of native carnivore ranges (Hilty and Merenlender 2004; Hilty et al. 2006), and the degradation of in stream spawning sites due to altered runoff and sediment loading (Lohse et al. 2008). Even the relocation of vineyards locally upslope adjacent to major viticulture areas has the potential to develop or degrade remaining interstitial natural areas surrounding vineyards. In novel areas, the pressure to convert remaining natural lands will increase as suitability declines in traditional wine grape growing regions, both within California and worldwide. Although many conscientious vintners within California incorporate principles of sustainability into their vineyard management, the conversion of natural lands to vineyards and the associated wine production and tourism infrastructure will likely result in additional fragmentation and degradation of remaining habitat (Merenlender 2000).

In areas of existing viticulture that are experiencing declining suitability, adaptation measures such as cooling vines through overhead sprinklers or additional irrigation may add further strain to already stressed water resources and associated freshwater ecosystems. Withdrawals for frost abatement within viticulture areas have been shown to result in up to 96 percent reduction of in-stream flows during cold-weather events (Dietch et al. 2009). An increase of withdrawals for extreme heat mitigation during dry summer months would also affect regional water resource management and planning.

The issue of shifting suitability for viticulture climates and the possible competition with conservation interests become amplified in the context of climate change – with both freshwater ecosystems and important areas for accommodating species range shifts potentially at odds with viticulture relocation or *in situ* adaptation measures. Unprotected natural areas with suitable climates for viticulture in future projections are at potential risk of conversion, especially considering the loss of optimal climates in many existing prime viticulture areas.

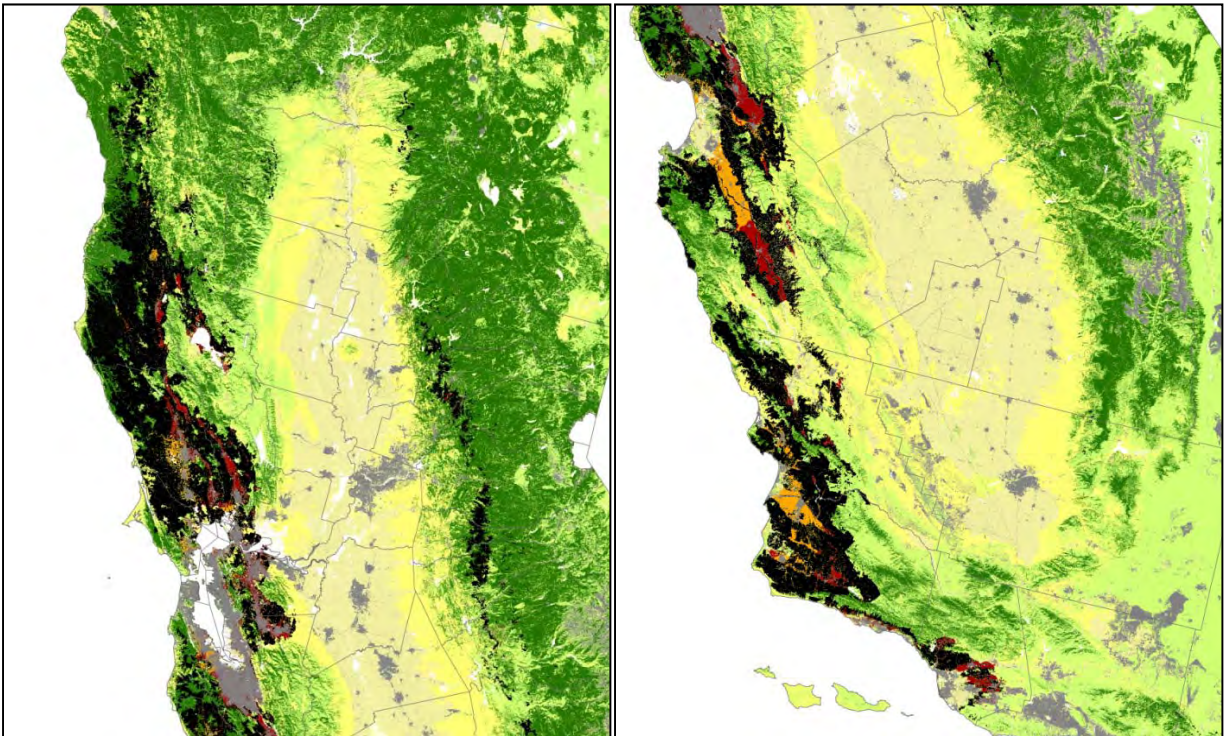


Figure 3.4: Potential Conflict of Natural Areas and Optimal Viticulture Climates. Areas where optimal viticulture climate modeled for all periods (Current, 2041–2070, and 2071–2100) intersects with National Land Cover Dataset (NLCD) 2001 undeveloped land shown in black. Suitable areas for viticulture that do not intersect with natural areas are shown as Current = Red; 2041–2070 = Orange; 2071–2100 = Blue. The left panel is the San Francisco Bay Area north to Humboldt County, and the right panel is the Bay Area south to Ventura County.

As optimal climates for viticulture shift under climate change, the total area that is climatically suitable within developed or non-natural lands (i.e., area with minimal conservation conflict) diminishes through time (Table 3.4). Additionally, for projections constructed on California-only occurrence points, the ratio of total optimal climate space that intersects with natural lands to climate space in non-natural lands increases from 2.3 in current climates to 5.8 by the end of the century.

Table 3.4: Summary of Climate Change Effects on the Total Optimal Viticulture Area in Non-natural Lands and the Ratio of Viticulture Climates in Natural to Non-natural Lands

	Viticulture Climate in Natural Areas Mid-century (% of present)	Viticulture Climate in Non-natural Areas Mid-century (% of present)	Viticulture Climate in Natural Areas End-century (% of present)	Viticulture Climate in Non-natural Areas End-century (% of present)	Ratio of Viticulture Climates in Natural to Non-natural Mid-century	Ratio of Viticulture Climates in Natural to Non-natural End-century
CA Points PCM A2	73.8	47.4	34.4	14.2	3.6	5.6
CA Points GFDL A2	48.9	39.6	9.1	3.6	2.9	5.8
Global Points PCM A2	118.6	93.2	79.4	77.1	2.2	1.8
Global Points GFDL A2	60.0	89.5	28.5	36.3	1.9	2.3

3.5 Conclusions

With significant areas of potential conflict between natural lands and the future distribution of optimal climates for viticulture, focused application of adaptation measures that limit additional water development and vineyard relocation will be important in mitigating stress on remaining natural lands. Several of these adaptation measures, such as vine orientation, trellising strategies to alter grape cluster insolation, and cooling through low-flow micro-misting technology are already being implemented. Furthermore, planning and management that recognizes this potential resource conflict under climate change will be essential to maximize the continued vitality of both California viticulture and natural ecosystems.

References

- Ackerly, David. 2009. "Evolution, origin and age of lineages in the Californian and Mediterranean floras." *Journal of Biogeography* 36: 1221–1233.
- Araujo, M. B., and A. Guisan. 2006. "Five (or so) challenges for species distribution modelling." *Journal of Biogeography* 33:1677–1688.
- Araujo, M. B., and M. New. 2007. "Ensemble forecasting of species distributions." *Trends in Ecology & Evolution* 22:42–47.
- Araujo, M. B., R. J. Whittaker, R. J. Ladle, and M. Erhard. 2005. "Reducing uncertainty in projections of extinction risk from climate change." *Global Ecology and Biogeography* 14:529–538.
- Calflora: Information on California plants for education, research and conservation. [web application]. 2009. Berkeley, California: The Calflora Database [a non-profit organization]. Available: <http://www.calflora.org/>. Accessed January 2011.
- Cayan, D. R., E. P. Maurer, M. D. Dettinger, M. Tyree, and K. Hayhoe. 2008. "Climate change scenarios for the California region." *Climatic Change* 87:S21–S42.
- CBI (The Conservation Biology Institute). 2010. Protected Areas – California. May 2010. Corvallis, Oregon, USA.
- Chaplin-Kramer, R. 2012. Climate Change and the Agricultural Sector in the San Francisco Bay Area: Changes in viticulture and rangeland forage production due to altered temperature and precipitation patterns. California Energy Commission. CEC-500-2012-033.
- CPAD. 2011. California Protected Areas Database Version 1.7 © September 2011 GreenInfo Network - www.calands.org.
- Deitch, M. J., G. M. Kondolf, and A. M. Merenlender. 2009. "Hydrologic impacts of small-scale instream diversions for frost and heat protection in the California wine country." *River Research and Applications* 25:118–134.
- Diffenbaugh, N. S., M. A. White, G. V. Jones, and M. Ashfaq. 2011. "Climate adaptation wedges: A case study of premium wine in the western United States." *Environmental Research Letters* 6.
- Elith, J., and C. H. Graham. 2009. "Do they? How do they? WHY do they differ? On finding reasons for differing performances of species distribution models." *Ecography* 32:66–77.
- Elith, J., C. H. Graham, R. P. Anderson, M. Dudik, S. Ferrier, A. Guisan, R. J. Hijmans, F. Huettmann, J. R. Leathwick, A. Lehmann, J. Li, L. G. Lohmann, B. A. Loiselle, G. Manion, C. Moritz, M. Nakamura, Y. Nakazawa, J. M. Overton, A. T. Peterson, S. J. Phillips, K. Richardson, R. Scachetti-Pereira, R. E. Schapire, J. Soberon, S. Williams, M. S. Wisz, and N. E. Zimmermann. 2006. "Novel methods improve prediction of species' distributions from occurrence data." *Ecography* 29:129–151.

- Flint L. E., and A. L. Flint. 2012. "Downscaling future climate scenarios to fine scales for hydrologic and ecological modeling and analysis." *Ecological Processes* 1: 1.
- Franklin, J. 2009. *Mapping Species Distributions: Spatial Inference and Predictions*. Cambridge University Press: Cambridge, United Kingdom.
- Gladstones, J. 1992. *Viticulture and Environment*. WineTitles: Adelaide.
- Gladstones, J. 2011. *Wine, Terroir and Climate Change*. Wakefield Press: Kent Town, South Australia, Australia.
- Grinnell J. 1924. *Animal life in the Yosemite*. University of California Press, Museum of Vertebrate Zoology: Berkeley, California, USA.
- Gurobi Optimization, Inc. 2011. Gurobi Optimizer Version 4.5 © 2011, Gurobi Optimization, Inc. www.gurobi.com.
- Hannah, L., G. Midgley, G. Hughes, and B. Bomhard. 2005. "The view from the cape. Extinction risk, protected areas, and climate change." *Bioscience* 55:231–242.
- Hannah, L. et al. 2007. "Protected area needs in a changing climate." *Frontiers in Ecology and the Environment* 5: 131–138.
- Hannah, L., C. Costello, C. Guo, L. Ries, C. Kolstad, D. Panitz, and N. Snider. 2011. "The impact of climate change on California timberlands." *Climatic Change* 109:429–443.
- Hayhoe, K., D. Cayan, C. B. Field, P. C. Frumhoff, E. P. Maurer, N. L. Miller, S. C. Moser, S. H. Schneider, K. N. Cahill, E. E. Cleland, L. Dale, R. Drapek, R. M. Hanemann, L. S. Kalkstein, J. Lenihan, C. K. Lunch, R. P. Neilson, S. C. Sheridan, and J. H. Verville. 2004. "Emissions pathways, climate change, and impacts on California." *Proceedings of the National Academy of Sciences of the United States of America* 101:12422–12427.
- Heller, N. E., and E. S. Zavaleta. 2009. "Biodiversity management in the face of climate change: A review of 22 years of recommendations." *Biological Conservation* 142:14–32.
- Hijmans, R. J., S. E. Cameron, J. L. Parra, P. G. Jones, and A. Jarvis. 2005. "Very high resolution interpolated climate surfaces for global land areas." *International Journal of Climatology* 25:1965–1978.
- Hilty, J. A., and A. M. Merenlender. 2004. "Use of riparian corridors and vineyards by mammalian predators in northern California." *Conservation Biology* 18: 126–135.
- Hilty, J. A., C. Brooks, E. Heaton, and A. M. Merenlender. 2006. "Forecasting the effect of land-use change on native and non-native mammalian predator distributions." *Biodiversity and Conservation* 15:2853–2871.
- Homer, C. C. Huang, L. Yang, B. Wylie and M. Coan. 2004. "Development of a 2001 National Landcover Database for the United States." *Photogrammetric Engineering and Remote Sensing* 70(7), July 2004. 829–840.
- Johnson, H., and J. Robinson. 2007. *The World Atlas of Wine 6th Edition*. Mitchell Beazley, London, UK.

- Jones, G. V., M. A. White, O. R. Cooper, and K. Storchmann. 2005. "Climate change and global wine quality." *Climatic Change* **73**: 319–343, doi:10.1007/s10584-005-4704-2.
- Kay, A. L., and H. N. Davies. 2008. "Calculating potential evaporation from climate model data. A source of uncertainty for hydrological climate change impacts." *Journal of Hydrology* **358**: 221–239.
- Keith, D. A., H. R. Akcakaya, W. Thuiller, G. F. Midgley, R. G. Pearson, S. J. Phillips, H. M. Regan, M. B. Araujo, and T. G. Rebelo. 2008. "Predicting extinction risks under climate change: Coupling stochastic population models with dynamic bioclimatic habitat models." *Biology Letters* **4**:560–563.
- Kelly, A. E., and M. L. Goulden. 2008. "Rapid shifts in plant distribution with recent climate change." *Proceeding of the National Academy of Sciences* **105**: 11823–26.
- Klausmeyer, K. R., and M. R. Shaw. 2009. "Climate Change, Habitat Loss, Protected Areas and the Climate Adaptation Potential of Species in Mediterranean Ecosystems Worldwide." *PLoS ONE* **4**: e6392.
- LaDochy, S., R. Medina, and W. Patzert. 2007. "Recent California climate variability: Spatial and temporal patterns in temperature trends." *Climate Research* **33**: 159–169.
- Loarie S., B. E. Carter, K. Hayhoe, S. McMahon, R. Moe, C. A. Knight, and D. Ackerly. 2008. "Climate change and the future of California's endemic flora." *PLoS ONE* **3**: e2502.
- Loarie, S. R., P. B. Duffy, H. Hamilton, G. P. Asner, C. B. Field, and D. D. Ackerly. 2009. "The velocity of climate change." *Nature* **462**:1052-U1111.
- Lobell, D. B., K. N. Cahill, and C. B. Field. 2007. "Historical effects of temperature and precipitation on California crop yields." *Climatic Change* **81**:187–203.
- Lohse, K. A., D. A. Newburn, J. J. Opperman, and A. M. Merenlender. 2008. "Forecasting relative impacts of land use on anadromous fish habitat to guide conservation planning." *Ecological Applications* **18**:467–482.
- Mawdsley, J. R., R. O'Malley, and D. S. Ojima. 2009. "A Review of Climate-Change Adaptation Strategies for Wildlife Management and Biodiversity Conservation." *Conservation Biology* **23**:1080–1089.
- Merenlender, A. M. 2000. "Mapping vineyard expansion provides information on agriculture and the environment." *California Agriculture* **54**(3):7–12.
- Midgley, G. F., L. Hannah, D. Millar, M. C. Rutherford, and L. W. Powrie. 2002. "Assessing the vulnerability of species richness to anthropogenic climate change in a biodiversity hotspot." *Global Ecology and Biogeography* **11**:445–451.
- Midgley, G. F., I. D. Davies, C. H. Albert, R. Altwegg, L. Hannah, G. O. Hughes, L. R. O'Halloran, C. Seo, J. H. Thorne, and W. Thuiller. 2010. "BioMove - an integrated platform simulating the dynamic response of species to environmental change." *Ecography* **33**:612–616.

- Moritz C., J. L. Patton, C. J. Conroy, J. L. Parra, G. C. White, and S. R. Bessinger. 2008. "Impact of a century of climate change on small-mammal communities in Yosemite National Park, USA." *Science* **322**: 261–64.
- NASS (National Agricultural Statistics Service). 2010. California Grape Crush Report 2010. California Department of Food and Agriculture and NASS California Field Office, Sacramento, California.
http://www.nass.usda.gov/Statistics_by_State/California/Publications/Grape_Crush/Final/2010/201003gcbbt00.pdf.
- Natural Resources Conservation Service, United States Department of Agriculture, Soil Survey Staff. U.S. General Soil Map (STATSGO2). Available online at <http://soildatamart.nrcs.usda.gov>. Accessed [January 10, 2011].
- Nemani, R. R., M. A. White, D. R. Cayan, G. V. Jones, S. W. Running, J. C. Coughlan, and D. L. Peterson. 2001. "Asymmetric warming over coastal California and its impact on the premium wine industry." *Climate Research* **19**:25–34.
- Parmesan, C. 2006. "Ecological and Evolutionary Responses to Recent Climate Change." *Annual Review of Ecology, Evolution, and Systematics* **37**: 637–69.
- Pearson, R. G., W. Thuiller, M. B. Araujo, E. Martinez-Meyer, L. Brotons, C. McClean, L. Miles, P. Segurado, T. P. Dawson, and D. C. Lees. 2006. "Model-based uncertainty in species range prediction." *Journal of Biogeography* **33**:1704–1711.
- Phillips, S. J., and M. Dudik. 2008. "Modeling of species distributions with Maxent: New extensions and a comprehensive evaluation." *Ecography* **31**:161–175.
- Phillips, S. J., P. Williams, G. Midgley, and A. Archer. 2008. "Optimizing dispersal corridors for the cape proteaceae using network flow." *Ecological Applications* **18**:1200–1211.
- Pfister, C. 1988. Variations in the spring-summer climate of central Europe from the High Middle Ages to 1850, in *Long and Short Term Variability of Climate*, H. Wanner, U. Siegenthaler (eds.). Springer-Verlag: Berlin, 57–82.
- PRISM Climate Group. Oregon State University. <http://prism.oregonstate.edu>.
- Randin, C. F., R. Engler, S. Normand, M. Zappa, N. E. Zimmermann, P. B. Pearman, P. Vittoz, W. Thuiller, and A. Guisan. 2009. "Climate change and plant distribution: Local models predict high-elevation persistence." *Global Change Biology* **15**:1557–1569.
- Seo, C., J. H. Thorne, L. Hannah, and W. Thuiller. 2009. "Scale effects in species distribution models: Implications for conservation planning under climate change." *Biology Letters* **5**:39–43.
- Stralberg D., D. Jonsomjit, C. A. Howell, M. A. Snyder, J. D. Alexander, J. A. Wiens, and T. L. Root. 2009. "Re-shuffling of species with climate disruption: A no-analog future for California's birds?" *PLoS ONE* **4**: e6825.
- Tabor, K., and J. W. Williams. 2010. "Globally downscaled climate projections for assessing the conservation impacts of climate change." *Ecological Applications* **20**:554–565

- Trivedi, M. R., P. M. Berry, M. D. Morecroft, and T. P. Dawson. 2008. "Spatial scale affects bioclimate model projections of climate change impacts on mountain plants." *Global Change Biology* **14**:1089–1103.
- Turner, W. R. et al. 2010. "Climate change: Helping nature survive the human response." *Conservation Letters* **3**: 304–312.
- USGS. 2011. US Geological Survey, Gap Analysis Program (GAP). February 2011. Protected Areas Database of the United States (PADUS), version 1.2.
- Vaudour, E. 2002. "The quality of grapes and wine in relation to geography: Notions of terroir at various scales." *Journal of Wine Research* **13**: 117–141.
- White, M. A., N. S. Diffenbaugh, G. V. Jones, J. S. Pal, and F. Giorgi. 2006. "Extreme heat reduces and shifts United States premium wine production in the 21st century." *Proceedings of the National Academy of Sciences of the United States of America* **103**:11217–11222.
- Wiens, J. A., D. Stralberg, D. Jongsomjit, C. A. Howell, and M. A. Snyder. 2009. "Niches, models, and climate change: Assessing the assumptions and uncertainties." *Proceedings of the National Academy of Sciences of the United States of America* **106**:19729–19736.
- Wine Institute with Data from U.S. Department of Commerce. World Wine Production by Country 2004-08 (2010).
- Winkler A. J., J. A. Cook, W. M. Kliwer, and L. A. Lider. 1974. *General Viticulture*. University of California Press: Berkeley, USA.
- Williams, J. W., and S. T. Jackson. 2007. "Novel climates, no-analog communities, and ecological surprises." *Frontiers in Ecology and the Environment* **5**:475–482.
- Williams, P. et al. 2005. "Planning for climate change: Identifying minimum-dispersal corridors for the Cape proteaceae." *Conservation Biology* **19**: 1063–1074. doi:10.1111/j.1523-1739.2005.00080.x.

Glossary

A2	business-as-usual scenario
AVA	American Viticulture Area
B1	assumes greenhouse gas abatement by mid-century
Bio_1	Annual Mean Temperature
Bio_10	Mean Temperature of Warmest Quarter
Bio_11	Mean Temperature of Coldest Quarter
Bio_12	Annual Precipitation
Bio_13	Precipitation of Wettest Month
Bio_14	Precipitation of Driest Month
Bio_15	Precipitation Seasonality (Coefficient of Variation)
Bio_16	Precipitation of Wettest Quarter
Bio_17	Precipitation of Driest Quarter
Bio_18	Precipitation of Warmest Quarter
Bio_19	Precipitation of Coldest Quarter
Bio_2	Mean Diurnal Range (Mean of monthly (max temp - min temp))
Bio_20	Cumulative Growing Degree Days above 5°C
Bio_22	Precipitation as snow
Bio_3	Isothermality (BIO2/BIO7) (* 100)
Bio_4	Temperature Seasonality (standard deviation *100)
Bio_5	Max Temperature of Warmest Month
Bio_6	Min Temperature of Coldest Month
Bio_7	Temperature Annual Range (BIO5-BIO6)
Bio_8	Mean Temperature of Wettest Quarter
Bio_9	Mean Temperature of Driest Quarter
°C	Celsius
CBI	The Conservation Biology Institute
CPAD	California Protected Area Database
DEM	digital elevation model
°F	Fahrenheit
GAP	U.S. Geological Survey's Gap Analysis Program
GCM	general circulation model
GDD	growing degree days
GFDL	Geophysical Fluid Dynamics Laboratory
IPCC	Intergovernmental Panel on Climate Change
IUCN	International Union for Conservation of Nature
km	kilometers
m	meters
mm	millimeters
NASS	National Agricultural Statistics Service
NFA	Network Flow Analysis

PADUS	Protected Areas Database of the United States
PCA	principal component analysis
PCM	Parallel Climate Model
PIER	Public Interest Energy Research
PRISM	Parameter-elevation Regressions on Independent Slopes Model
RD&D	research, development, and demonstration
SDM	species distribution models
SRES	Emissions Scenarios
STATSGO2	State Soil Geographic database
UC	University of California
USGS	United States Geological Survey